Quaternary Science Reviews 221 (2019) 105872

Contents lists available at ScienceDirect

Quaternary Science Reviews

journal homepage: www.elsevier.com/locate/quascirev

Hydro-climate research of the late quaternary of the Eastern Mediterranean-Levant region based on speleothems research – A review

M. Bar-Matthews [a, *], J. Keinan [a, b], A. Ayalon [a]

[a] Geological Survey of Israel, Yisha'ayahu Leibowitz St. 32 St, Jerusalem, Israel
[b] Institute of Earth Sciences, The Hebrew University, Jerusalem, 91904, Israel

ARTICLE INFO

Article history:
Received 31 December 2018
Received in revised form
6 August 2019
Accepted 8 August 2019
Available online xxx

Keywords:
Paleoclimate
Dead Sea Basin
Glacials
Marine Isotope Stage 5e
Sapropels
Speleothems

ABSTRACT

The Eastern Mediterranean (EM) - Levant region is the eastern borderland of the Eastern Mediterranean Sea (EMS). The EMS brings Mediterranean climate zones to the immediate coastal region and hinterland, but away from the influence of the EMS, the region rapidly becomes a desert. Paleoclimate evidence derived from a large number of studies on speleothems from caves located along sharp climatic gradients enables deep insight into the climate in the EM-Levant region. Growth periods and isotopic composition of speleothems from the various climate regimes capture the regional signals of temperature, rainfall amount and vegetation.

Speleothems from northern and central Israel grew continuously in areas where present-day annual rainfall is ~400–500 mm and show that water was always available during glacials and interglacials. These speleothems display a well-defined $\delta^{18}O$ orbital modulation of glacial and interglacial marine isotope stages (MIS) and show good correlations with the EMS marine records, pointing to strong direct sea-land links. The climatic record indicates relatively drier and cooler glacials but extreme wet peaks during interglacials, mainly MIS 5e between 128–120 ka BP. Pluvial conditions penetrated to the northern, central and southern Negev Desert.

The present-day climatic gradient between the different climatic regions existed through interglacials. However, growth periods of speleothems from the northern Negev Desert, from the "rain shadow' desert, and the Dead Sea Basin, suggest that during last glacial the desert boundary moved from its interglacial and present-day position ~30 km farther south and ~60 km farther east, due to positive water balance.

1. Introduction

1.1. Present-day climatic conditions

This review presents a summary of the hydro-climate of the Eastern Mediterranean (EM) - Levant region based on speleothems records during glacial and interglacials, with particular emphasis on Marine Isotopic Stage (MIS) 5e.

The EM - Levant region (Fig. 1) lies at the geographical meeting point of Eurasia, Africa, the Mediterranean Sea, and the Indian Ocean. The region is located along the Eastern Mediterranean Sea (EMS), which defines the Mediterranean climate zones. Away from the climatic influence of the EMS, the region rapidly becomes a desert.

The review emphasizes the importance of studying several caves in rather small area, along sharp climatic gradient, in order to establish the full range of paleoclimate conditions that prevailed in mid-low latitude regions located under the influence of the EMS on one hand, and to the larger Saharo-Arabian Desert on the other hand.

The caves studied are located along N–S and W-E transects of the EMS-Levant region. The N–S transect (Fig. 1) starts from Mt. Lebanon and Mt Hermon in the northern Levant with present-day annual rainfall of more than 800 mm, across northern and central Israel with annual rainfall ranging from ~800 mm to ~500 mm, through the northern Negev Desert with annual rainfall of ~300 mm to the central and southern Negev Desert with ~100 to less than 50 mm annual rainfall. This latter region links the Levant

* Corresponding author.
E-mail address: matthews@gsi.gov.il (M. Bar-Matthews).

https://doi.org/10.1016/j.quascirev.2019.105872
0277-3791/

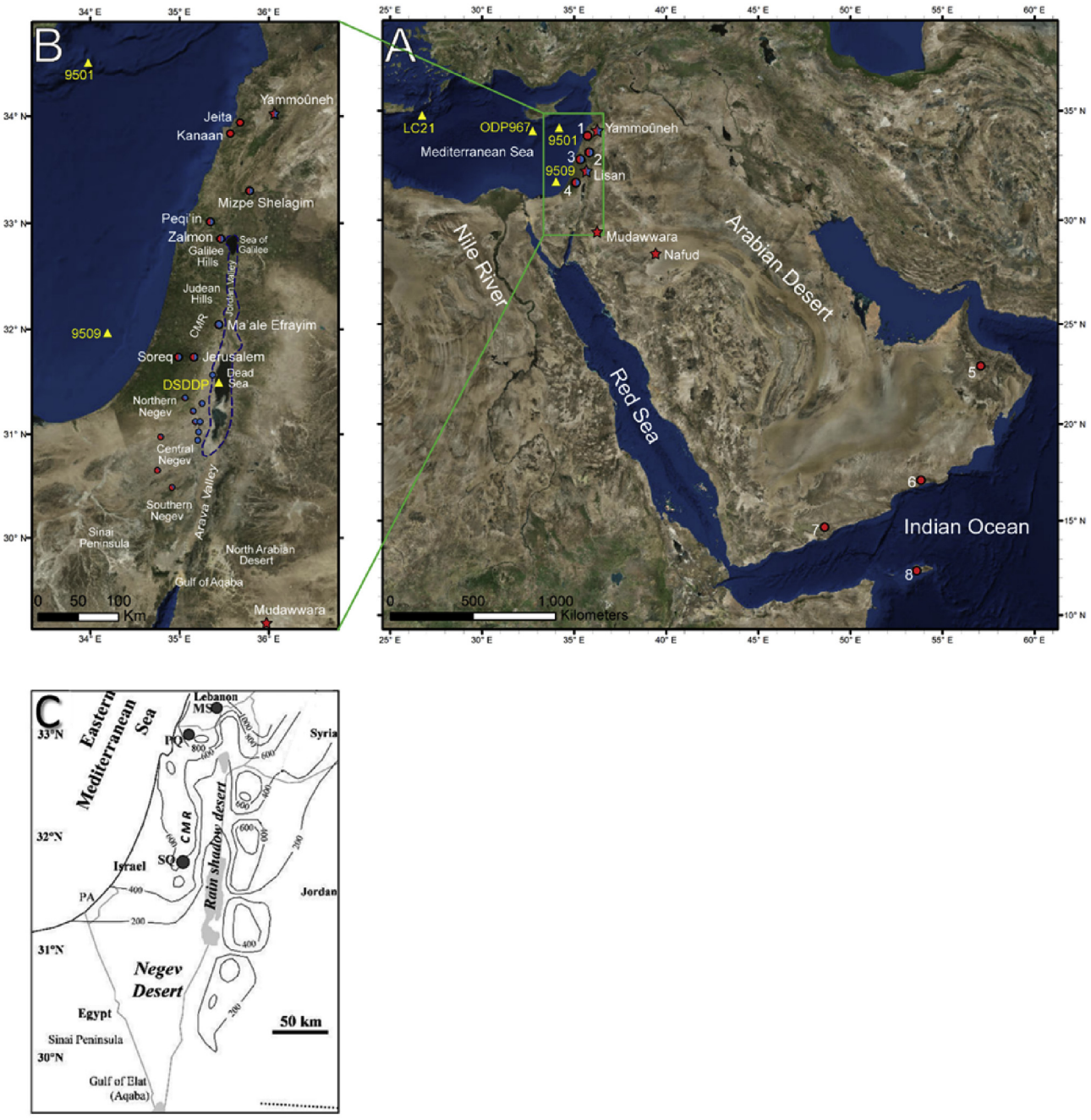

Fig. 1. Regional maps (A and B, C) with locations of the Levant study sites described in the text (B and C are enlargements of the green rectangular area in A). Caves are shown as filled circles, marine drilled core sites as yellow triangles, and lakes as stars. Study sites are color-coded: blue – "wet" during glacial periods, red – "wet" during interglacial periods. The dashed blue line in B marks the highest stand of Lake Lisan (modified after Torfstein et al., 2013). In A, the following caves are numbered: 1-Jeita and Kanaan caves (Cheng et al., 2015; Nehme et al., 2015; Verheyden et al., 2017) 2-Mizpe Shelagim Cave (Ayalon et al., 2013), 3-Peqi'in (Bar-Matthews et al., 2003) and Zalmon caves (Keinan et al., 2019), 4-Soreq (e.g. Bar-Matthews et al., 1997) and Jerusalem caves (Frumkin et al., 1999), 5-Hoti Cave (e.g., Burns et al., 1998), 6-Qunf and Defore caves (Fleitmann et al., 2007), 7-Mukallah Cave (Fleitmann et al., 2011), 8-Dimarshim Cave (Fleitmann et al., 2007). B shows a number of caves and geographical features described in the text. C. indicates the present-day isohyets. Mizpe Shelagim, Peqi'in and Soreq caves are shown as MS, PQ and SQ respectively. The Central Mountain Ridge of Israel is marked as CMR in B and C.

with North Africa and defines the northeastern corner of the Sahara Desert. The W-E transect is based on speleothems from caves located both on the western flanks and the "rain shadow" desert on the eastern side of the Central Mountain Ridge (CMR) of Israel, along the Dead Sea Basin (DSB), with present-day annual rainfall varying from ~500 mm in the northern segment, to less than 50 mm in the southern segment (Fig. 1).

1.2. Origin and isotopic composition of rainfall

Rain is the source of water for speleothem growth and therefore the rainfall patterns play an important role in the occurrence of speleothems. The main rainfall precipitating atmospheric patterns in the northern Levant-EM region are extratropical winter (October–April) EM cyclones, the Cyprus Lows, with rainfall fronts that originate in the North Atlantic Ocean and the Mediterranean Sea

and their storm tracks frequently pass over Europe and the Mediterranean Sea (Rindsberger et al., 1983; Sharon and Kutiel, 1986; Kushnir et al., 2017). December to February are the wettest months. The cold dry air masses originating in the Atlantic Ocean take up their moisture from the warm EM sea surface. The humidity gradient in this process defines a unique relationship between the isotopic composition of hydrogen (δD) and oxygen ($\delta^{18}O$) in rainfall referred to as the Mediterranean Meteoric Water Line (MMWL). The MMWL features high d-excess values (d excess = $\delta D - 8^{*}\delta^{18}O$) of 20–30‰ relative to the global d-excess of 10‰ (Rindsberger et al., 1983; Gat and Carmi, 1987; Rozanski et al., 1993; Gat, 1996; Ayalon et al., 1998; Matthews et al., 2000; McGarry et al., 2004). Locally, the variations in the stable isotope composition of precipitation depend on temperature, distance from the sea (continental effect), elevation, precipitation amount, and air mass trajectory (Rindsberger et al., 1983; Bar-Matthews et al., 1997, 2003 Ayalon et al., 2004). The amount of precipitation is generally higher in northern Israel and in the west-facing mountain slopes. The correlation between rainfall amount and its mean annual $\delta^{18}O$ based on empirical studies shows a decrease of ~1‰ for ~250 mm (Ayalon et al., 1998, 2004: Bar-Matthews et al., 2003; Orland et al., 2009).

The main moisture source to the Israeli deserts is currently the EM low-pressure system. Sometimes this system is pulled south by EM lows related to the Active Red Sea Troughs (e.g., Kahana et al., 2002; Sharon and Kutiel, 1986; Tsvieli and Zangvil, 2007). These smaller southern sources are unrelated to the summer southwest Indian and East African monsoons. These rainfall tropical plumes (TPs) usually do not precipitate rain across the entire eastern Sahara, but only where they interact with the south-westerly subtropical jets over eastern Egypt, Sinai, northern Arabia, and the Negev Desert (Ziv, 2001; Kahana et al., 2002; Rubin et al., 2007). They are responsible for some of the largest floods in the area (Kahana et al., 2002).

Water availability for recharge and runoff in the region, reflects the balance between precipitation, evaporative loss to the atmosphere, and runoff into the sea. The calculated portion of the available water budget in the EM climate region recharging the aquifers is ~25–30% (Ayalon et al., 2004; Gvirtzman, 2002), while the remaining 70% is lost by runoff, evaporation and evapotranspiration. Most recharge and runoff follow periods of heavy rainfall, when the available water exceeds the capacity of soil and epikarst to store the water. Predicting future rainfall precipitation amounts in the Middle East and North Africa is difficult because of the high natural variability of modern precipitation, which is mainly due to global climate change but also reflects topographic variations and distance from the Mediterranean coastline (e.g., Lionello et al., 2006; Enzel et al., 2008; Terink et al., 2013).

2. Paleoclimate-paleohydrology of the EM – Levant region based on the speleothems record

Speleothems are important archives for the reconstruction of continental paleoclimates, paleoenvironment and paleohydrology. They can be accurately dated by the uranium–thorium isotopic method; thus it is possible to accurately determine their growth and non-growth (hiatus) periods as indicators of water availability on land. Speleothems grow in caves when water reaches the unsaturated zone, but they do not grow in the water-depleted conditions of arid/hyperarid deserts, and under freezing conditions (e.g., Fleitmann et al., 2003; Vaks et al., 2003, 2007; 2010, 2014; Ayalon et al., 2013). In semi-arid and arid environments, speleothem deposition indicates positive effective precipitation (i.e., the difference between precipitation and evaporation-runoff), thus enabling precise tracing of past humid episodes in the present-day desert region. Together with the isotopic compositions of oxygen ($\delta^{18}O$) and carbon ($\delta^{13}C$) of each dated laminae, it is possible to reconstruct the regional paleoclimate (e.g., Bar-Matthews et al., 2000, 2003; 2017; Vaks et al., 2003, 2007; 2010; Fleitmann et al., 2011; Frumkin et al., 2011; Verheyden et al., 2017). The relatively large number of studies made on speleothems from caves in the EM-Levant region, allow us to achieve a deep insight into the climate of the land region; covering almost the entire climatic transect from the relatively wet EM region receiving >800 mm annual rainfall, to the extremely dry region of Northeast Africa.

This review is based on the following cave sites (Fig. 1):

2.1. Caves location

2.1.1. Caves from the Northern Levant

- Jeita and Kanaan caves (Jeita Cave located ~15 km north of Beirut and Kanaan Cave ~5 km south of Jeita Cave) located on the western flank of central Mount Lebanon at ~100 m above sea level and 2–5 km from the EMS coastline. The caves sites are strongly influenced by the maritime Mediterranean climate receiving ~800 mm of annual rainfall (Cheng et al., 2015; Nehme et al., 2015; Verheyden et al., 2017).
- Mizpe Shelagim (MS) Cave in Mt Hermon, 2224 masl, receives annual precipitation of 1000–2000 mm, primarily as snowfall in December–March. This region is the southernmost point of the Alpine-type karst that extends from Turkey to Syria and Lebanon (Ayalon et al., 2013).

2.1.2. Cave from northern and central Israel

- Peqi'in Cave is located in the Upper Galilee, northern Israel, at 650 masl and 25 km from the EMS. The climate is semi-arid to sub-humid Mediterranean, average annual precipitation ~650 mm with rain occurring only in the winter months (Bar-Matthews et al., 2003).
- Soreq and Jerusalem caves in the Judea Mountains (at 400 m and 730 masl, respectively) are on the west-facing slope of the Central Mountain Ridge (CMR) of Israel, which runs roughly parallel to the EMS coastline, approximately 40–60 km inland. Average annual precipitation ~500–600 mm (Bar-Matthews et al., 1997, 1998; 2003; Ayalon et al., 1998, 1999; 2002; Frumkin et al., 1999).

2.1.3. Cave from the northern Negev Desert

- Two caves from the mildly arid northern Negev Desert: an approximately 40 km wide belt between the 350 and ~150 mm isohyets. The northern Negev Desert is the southern boundary of the Mediterranean climate zone (Vaks et al., 2006).

2.1.4. Caves from central and southern Negev Desert

- Nine caves in the Negev Desert from the arid and hyper-arid central and southern Negev, along north-south transect from 150 mm to less than 50 mm annual rainfall.

The southern Negev Desert defines the North-East corner of the Sahara Desert, with 150–25 mm annual rainfall (Vaks et al., 2010).

2.1.5. Caves from the Dead Sea 'rain shadow' region

The region lies east of the mild Mediterranean climate and defines a 15–30 km wide north–south strip along the DSB and the

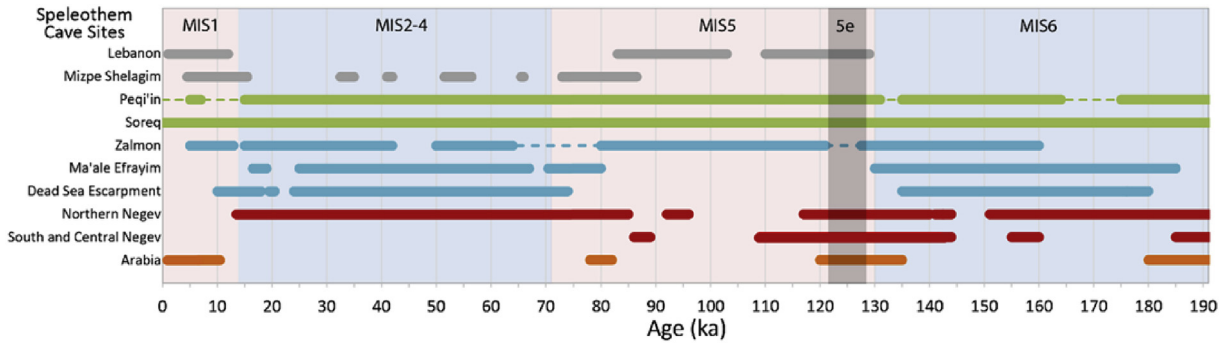

Fig. 2. Depositional periods at the cave sites described in the text. Lebanon (Cheng et al., 2015; Nehme et al., 2015; Verheyden et al., 2017); Mizpe Shelagim (Ayalon et al., 2013) Peqi'in and Soreq (Bar-Matthews et al., 2003), Zalmon (Keinan et al., 2019), Ma'ale Efrayim (Vaks et al., 2003), Dead Sea Escarpment (Lisker et al., 2010); Northern Negev (Vaks et al., 2006), South and Central Negev (Vaks et al., 2010), Arabia including Northern and Southern Oman, and Socotra Island, Yemen (Fleitmann et al., 2007, 2011). Light blue/pink fields represent glacial/interglacial periods. MIS periods are taken from Lisiecki and Raymo (2005). MIS 5e is shown as a grey rectangle. The brighter red line for South and Central Negev marks intensive speleothem deposition (after Vaks et al., 2010).

Jordan Valley.

- Zalmon Cave, located in the northern part of the DSB, approximately 8 km west of the Sea of Galilee, ~23 m above sea level and is ~35 km east of the EMS. The climate in the region is Mediterranean, with average annual precipitation of ~550 mm and an annual temperature average of 21 °C (Keinan et al., 2019).
- Ma'ale Efrayim (ME) Cave, located 250 masl near the Jordan Valley, and 60 km inland from the EMS. Average annual rainfall 200–300 mm and mean annual temperature of 21–22 °C (Vaks et al., 2003).
- Relict karstic caves along the Dead Sea Fault Escarpment (Lisker et al., 2009, 2010).

2.1.6. Caves from southern Arabia and Yemen

- Four caves from southern Arabia Peninsula in present-day semi-arid – arid conditions receiving rainfall from the Indian Ocean monsoon system (e.g., Burns et al., 1998, 2001; Fleitmann et al., 2003, 2007, 2011).

2.2. Glacial and interglacial conditions in central and northern Israel (Judea and Galilee mountains)

Speleothems deposition in northern and central Israel was continuous during both glacials and interglacials (Ayalon et al., 1998, 1999; 2002; Bar-Matthews et al., 1997, 1998; 2000, 2003; Frumkin et al., 1999; and Figs. 2 and 3). This continuity implies that annual rainfall during interglacial was always more than ~300 mm and during glacials more than ~250 mm (Vaks et al., 2006, 2010).

The detailed speleothems work made on Soreq and Peqi'in caves in central and northern Israel respectively, show important features that characterize their $\delta^{18}O$ and $\delta^{13}C$ values during two glacial periods MIS 6 and MIS 4–2 and two interglacial periods MIS 5 and MIS 1 (Fig. 3) that emphasize the fact that the speleothems capture the regional signal of temperature, rainfall and vegetation isotopic composition (Bar-Matthews et al., 2003) as described below.

Soreq and Peqi'in caves speleothems $\delta^{18}O$ display a well-defined orbital modulation between and among glacial and interglacial marine isotope stages (MIS) (Fig. 3) and show good correlation with the EMS foraminiferal records (Fig. 4). Superimposed on the glacial – interglacial cycles are repeated oscillations on millennial and even shorter time scales. The speleothems $\delta^{18}O$ records have been

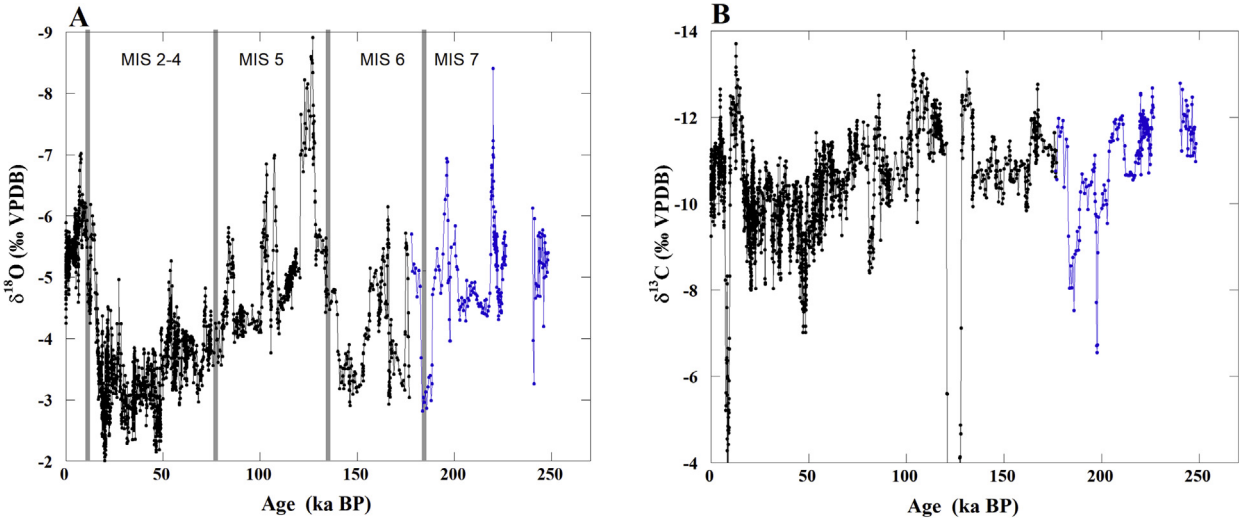

Fig. 3. $\delta^{18}O$ (A) and $\delta^{13}C$ (B) records of speleothems from central (Soreq Cave black, 0–180 ka) and northern Israel (Peqi'in Cave blue, 180–240 ka) during the last 240 ka (modified from Bar-Matthews et al., 2003; Grant et al., 2012). The vertical bars in A indicate the Marine Isotope Stages (MIS).

compared with the $\delta^{18}O$ record of the *G. ruber* from several cores in the EMS (Fig. 1): marine core 9501, taken SE of Cyprus, representing the northern Levantine Basin, marine core 9509, located ~380 km farther south, represents the southeastern Levantine Basin in an area influenced by the River Nile plume (Almogi-Labin et al., 2009), marine core LC-21 from the southeast Aegean Sea (Grant et al., 2012, 2016) and this review, and marine core ODP 967, south of Cyprus, at the base (2550 masl) of the northern slope of the Eratosthenes Seamount (Emeis et al., 1998). The $\delta^{18}O$ *G. ruber* records from all these sites display a well-defined orbital modulation of glacial and interglacial MIS events and also show good correlation with some shorter scale climatic events, such as Heinrich events and Dansgaard- Oeschger (D- O) cycles and North Greenland Ice Core Project (NGRIP) temperatures (Emeis et al., 1998, 2000a, b, 2003; Rohling et al., 2002; Almogi-Labin et al., 2009; Grant et al., 2012, 2016). These correlations emphasize the link between Northern Hemisphere climate change and the climate of the EMS (Marino et al., 2009). However, although the EMS marine record follows the global pattern, it is characterized by larger $\delta^{18}O$ variations (Fontugne and Calvert, 1992; Kallel et al., 1997a,b; Almogi-Labin et al., 2009). The large glacial - interglacial shift in $\delta^{18}O$ values reflects not only the ice-volume effect and sea level changes, but to a considerable extent, the amplification of climate change effects in the semi-enclosed continental conditions of the EMS. This amplification is due to the contribution of significant inflow of ^{18}O-depleted water carrying monsoonal signal into the EMS during peak interglacial through the Nile River and other rivers from North Africa (e.g., Rossignol-Strick, 1985; Fontugne and Calvert, 1992; Emeis et al., 1998; Osborne et al., 2008; Almogi-Labin et al., 2009) together with enhanced hydrological conditions in the entire EM basin (e.g. Kallel et al., 1997a; b; Bar-Matthews et al., 2000; Bar-Matthews, 2014). This is evident from the 5.0‰ shift in the $\delta^{18}O$ values of *G. ruber*, surface-dwelling planktonic foraminifera which is widely used for reconstructing ice volume, sea level changes, temperature, and salinity, in the EMS. *G. ruber* $\delta^{18}O$ values range from ~-2‰ during peak interglacial to about +3.0‰ during peak glacials, compared with 2‰ variations in the western Mediterranean Sea. The speleothems show similar large $\delta^{18}O$ variations. The overall good matching of $\delta^{18}O$ between the speleothems and the EMS marine record, and the similar differences between the speleothems and the *Globigerinoides ruber (G. ruber)* ($\Delta\delta^{18}O_{\text{sea-land}}$) between marine cores LC21, 9501 and $\delta^{18}O$ of Soreq Cave speleothems, with an average of 5.7 ± 0.7‰ (Fig. 4), establishing a robust link between the land and sea, demonstrating the importance of the source effect on the speleothems $\delta^{18}O$ (Bar-Matthews et al., 2000, 2003; Kolodny et al., 2005; Almogi-Labin et al., 2009; Grant et al., 2012).

It follows that interpretation of the $\delta^{18}O$ speleothems record of central and northern Israel must take into consideration the EMS surface record. $\Delta\delta^{18}O_{\text{sea-land}}$ would have remained constant if the source effect were the only control of rainwater $\delta^{18}O$. However, the short time oscillation super-imposed on the glacial-interglacial modulation (Fig. 4), most probably reflects local and regional climatic variations (Almogi-Labin et al., 2009; Grant et al., 2016). The influence of temperature change, rainfall amount, sea-land distance, and elevation changes must therefore be taken into consideration. The most positive $\Delta\delta^{18}O_{\text{sea-land}}$ values found during peak glacial periods were suggested to reflect bigger sea-land $\delta^{18}O$ fractionations due to enhanced Rayleigh distillation processes in the cloud-rainfall system resulting from the larger sea and land distance and elevation differences at low glacial sea levels (Almogi-Labin et al., 2009). In order to deconvolve the local EM climate signal from any bias related to monsoon/riverine runoff, Grant et al. (2016) calculated the 'Soreq excess $\delta^{18}O$' ($\delta^{18}O_{\text{SOREQ XS}}$) by subtracting the LC21 $\delta^{18}O_{\text{G.ruber}}$ record from the Soreq Cave speleothems $\delta^{18}O$ record. They eliminated glacial cycles from their calculations. In this review we applied the same approach for the last 140 ka BP including glacial intervals (Fig. 4C). Throughout most of last glacial the residual ($\delta^{18}O_{\text{SOREQ XS}}$) is positive (Fig. 4C), supporting much colder and dryer conditions during most of last glacial in the region. Very frequent alternations between positive and negative values characterize the deglaciation.

The combined $\delta^{18}O$-$\delta^{13}C$ record of the speleothems together with other proxies such as their petrographic characteristics, fluid inclusions, and Δ_{47} ('clumped isotopes'), enable to better construct the regional climatic conditions and how the land record adjacent to the EMS response to changes in the EMS source variations.

2.2.1. Glacial conditions in central and northern Israel

During the previous glacial MIS 6 (185–135 ka BP) $\delta^{18}O$ values fluctuate between ~ -6.0‰ and ~-3.0‰ (Fig. 3). Despite the large $\delta^{18}O$ variations, $\delta^{13}C$ values remain almost constant between ~ -12.0‰ and −10.0‰ suggesting domination of C3 type vegetation throughout the entire time interval (Ayalon et al., 2002). A more complicated pattern characterizes most of the last glacial, MIS 4–2 (78–19 ka BP), with $\delta^{18}O$ fluctuations between ~ -5.0‰ and −2.0‰ and $\delta^{13}C$ values varying between ~ -11.0‰ and −7.0‰, implying that there were changes in vegetation type from Mediterranean C3 type vegetation to a mixed C3 and C4 type. However, such rises in $\delta^{13}C$ values may be also explained by dominance of C3 type vegetation under conditions of enhanced stress due to colder temperatures and/or reduced rainfall (Bar-Matthews et al., 2003). The relatively higher $\delta^{18}O$ and $\delta^{13}C$ values during most of last glacial, compared with MIS 6, suggest that climate conditions during the last glacial generally were colder. There is evidence to indicate that the last glacial was cold: the relatively high $\delta^{18}O$ and $\delta^{13}C$ values combined with calculated temperatures in Soreq Cave area of ~10 °C during the Last Glacial Maximum (LGM) and up to 14–16 °C throughout most of the glacial. These values are based on fluid inclusions (δD) of water trapped in the speleothems (Matthews et al., 2000; McGarry et al., 2004), and the Δ_{47} temperatures (Affek et al., 2008).

Similar ranges of temperatures were calculated also for the EM Sea Surface Temperatures (SST) based on alkenones and Mg/Ca ratios of foraminifera. Such calculated temperatures during the LGM are 11–12 °C (compared to present-day mean annual temperature of 18 °C), and temperatures throughout most of the last glacial period varied between 13 °C and 16 °C (Emeis et al., 1998, 2000b; 2003; Essallami et al., 2007; Almogi-Labin et al., 2009). These cool periods are associated with low Arboreal Pollen (AP) and with high values of semi-desert and desert vegetation (Cheddadi and Rossignol-Strick, 1995a, 1995b; Langgut et al., 2011).

A significantly warmer and wetter interval occurred during the last glacial between ~55–52 ka BP, which coincides with the insolation maximum in the Northern Hemisphere and the D - O interstadial 14. This time period is characterized by relatively low $\delta^{18}O$ and $\delta^{13}C$ values of the speleothems (Fig. 3), which is also evident in the EMS marine record in lower values of *G. ruber* $\delta^{18}O$ (Almogi-Labin et al., 2009 and Fig. 4) and higher percentage of Arboreal Pollen and evergreen oak that points to increased humidity (Fig. 5) (Langgut et al., 2011, 2018). This time interval also coincides with increased low-latitude hydrological activity when the EMS experienced marked pluvial conditions (Rossignol-Strick et al., 1982; Rossignol-Strick, 1985; Hilgen, 1991; Cheddadi and Rossignol-Strick, 1995a, 1995b; Lourens et al., 1996; Bar-Matthews et al., 2000; Langgut et al., 2011, 2018), possibly associated with the missing sapropel "S2″ whose existence is controversial (Cita et al., 1977). Interestingly, in Manot Cave (north-west Israel) there is evidence for the expansion of modern humans of African origin dated at 54.7 ± 5.5 ka BP that most probably reflects the last main

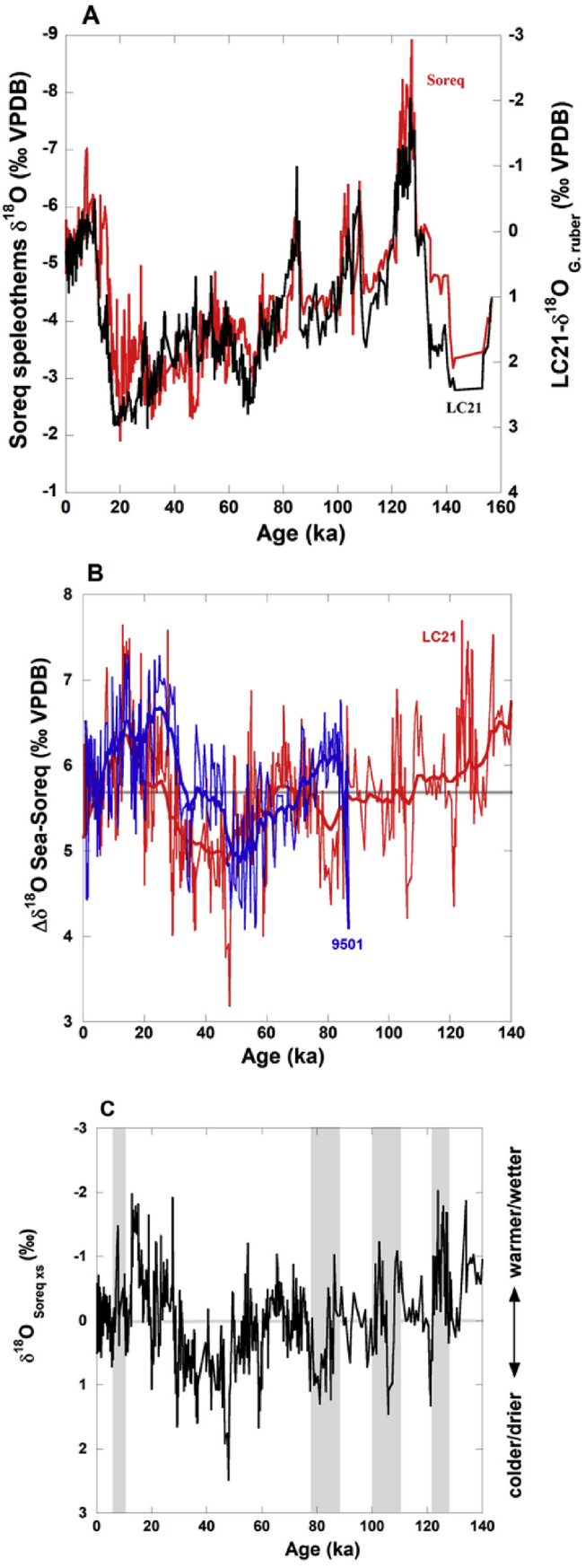

Fig. 4. A. Comparison of Soreq Cave $\delta^{18}O$ isotopic profile (red) and EM planktonic foraminiferal (*G. ruber*) $\delta^{18}O$ record from marine core LC21 (black; Grant et al., 2012, 2016). B. $\Delta\delta^{18}O_{sea-land}$ values, documented by the difference between $\delta^{18}O$ of the planktonic foraminifera *Globigerinoides ruber* $\delta^{18}O$ values from marine core LC21in red and marine core 9501 in blue (Almogi-Labin et al., 2009) and Soreq Cave speleothems. Superimposed is the three point moving average. The horizontal gray line marks the average of the $\Delta\delta^{18}O_{sea-land}$ of 5.7‰. C. Soreq Cave 'excess' ($\delta^{18}O_{Soreq\ xs}$ ‰) for the last 140 ka (see Grant et al., 2016). Sapropel periods are marked in grey rectangles. '

'out of Africa' migration due to warmer and wetter climatic conditions over the Northern Sahara and the Mediterranean (Hershkovitz et al., 2015).

The overall paleoclimate picture is derived also from lacustrine sediment sequence, the Yammoûneh paleolake (Fig. 1), a small karstic basin in Lebanon, located at 1360 m above sea level on the eastern flanks of Mt. Lebanon, 37 km from the Mediterranean shoreline (Develle et al., 2010, 2011). Although the record suffers from chronological uncertainties, a combination of proxies including pollen, sediment properties, and isotope record point to generally colder and dry last glacial conditions (Develle et al., 2010, 2011), apart from two pluvial episodes that may be correlative within error to the pluvial period between 55–52 ka BP. The Yammoûneh data also show also that the previous glacial, MIS 6, was wetter than the last glacial, similar to the conclusions derived from the speleothems record (Ayalon et al., 2002).

2.2.2. Interglacial conditions central and northern Israel

The transition from glacial MIS 6 to MIS 5 occurs in two major steps (Fig. 3). The first step from ~141–134 ka BP occurs when $\delta^{18}O$ decreases from ~-3.4‰ to ~ -4.7‰ and the second step from 134 to 128.5 ka BP with a further $\delta^{18}O$ decrease to ~ -5.5‰ and $\delta^{13}C$ decrease from ~-10.5‰ to ~ -12.5‰. The entire MIS 5 period is characterized by large $\delta^{18}O$ fluctuations (Fig. 3). The lowest values occur during three sub-stages, 128 and 120 ka BP (MIS 5e), between 109–100 ka BP (MIS 5c) with a short three ka period with less negative values, and between 86-83 ka BP (MIS 5a). The very low $\delta^{18}O$ values coincide with the low EMS *G. ruber* $\delta^{18}O$ values and with the timing of the deposition of sapropel layers, which are unique organic-rich sediments. The lowest $\delta^{18}O$ *G. ruber* values typically found in sapropel layers are indicative of surface freshwater contribution. The sapropel layers indeed were deposited during cycles of extreme wet periods with enhanced rainfall over the Mediterranean basin (Kallel et al., 1997a; b), and large amounts of freshwater input from North African Monsoon (Rodríguez-Sanz et al., 2017). Rodríguez-Sanz et al. (2017) argue that during early MIS 5, between ~134–128 ka BP, the additional freshwater was mainly derived from the North Atlantic source, whereas between ~128–120 ka BP monsoon-driven flooding originated from Nile River flow and from freshwater originating in the central Saharan mountain ranges (e.g., Scrivner et al., 2004; Osborne et al., 2008, 2010; Rodríguez-Sanz et al., 2017). 'Clumped isotope' (Δ47)-based temperatures of marine core ODP967 and LC21 indicate that EMS surface temperatures were consistently higher by ~7 ± 4 °C than late-Holocene temperatures (Rodríguez-Sanz et al., 2017), due to 30% thinning of the summer mixed layer at the S5 onset.

The interglacial pollen assemblage points to the dominance of evergreen and deciduous trees, with Mediterranean vegetation and temperate trees (Fig. 5) indicating warm and wet conditions (e.g., Rossignol-Strick, 1983, 1985; Cheddadi and Rossignol-Strick, 1995a, 1995b; Kotthoff et al., 2008; Langgut, 2008; Langgut et al., 2011). Rohling et al. (2015 their Fig. 7) calculated the residuals, (i.e., difference between Soreq Cave values and LC21 values) for each of the well-expressed sapropels and found negative offsets that broadly indicate warmer/wetter conditions at Soreq Cave. They also noted increases in regional humidity to be more pronounced during S5 and mainly in the later portion.

Winter climate modelling of the interglacial insolation maxima

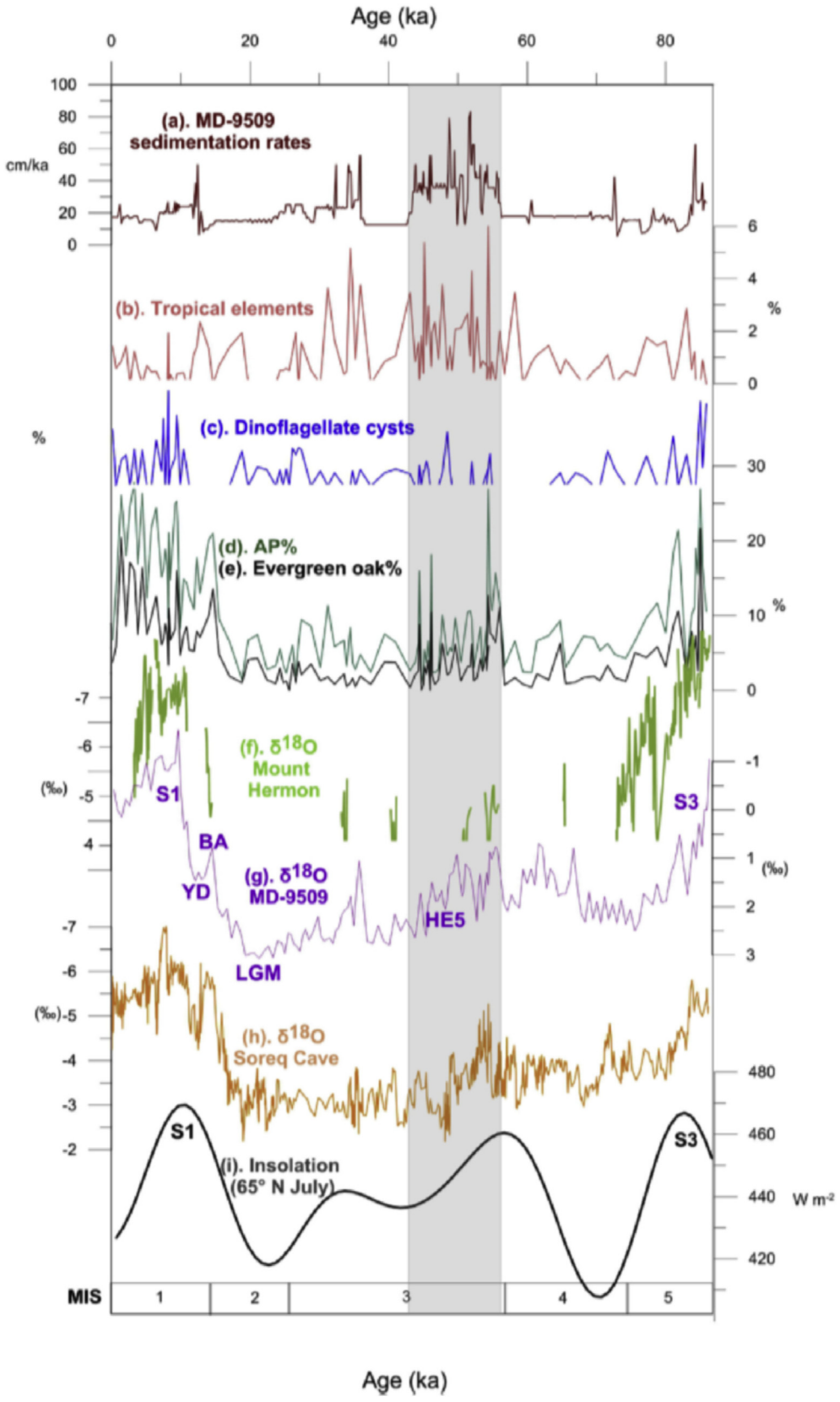

Fig. 5. Representative paleoenvironmental records with emphasis on the southern part of the EM-Levant region: a) Core MD-9509 sedimentation rates (Langgut et al., 2011); b) Core MD-9509 tropical elements (Langgut et al., 2018); c) Core MD-9509 dinoflagellate cysts (Langgut et al., 2018); d) Core MD-9509 total arboreal pollen (AP) excluding bisaccate coniferous pollen; e) Core MD-9509 evergreen oak (Quercus calliprinos type); f) $\delta^{18}O$ values of Mount Hermon speleothems (Mizpe Shelagim Cave; Ayalon et al., 2013); g) $\delta^{18}O$ values of the planktonic foraminifera *Globigerinoides ruber* of core MD-9509 (Almogi-Labin et al., 2009); h) $\delta^{18}O$ values of Soreq Cave speleothems (Bar-Matthews et al., 2003); i) Insolation (65°N July): peaks are associated with North African humid periods and the accumulation of sapropels S1 and S3 in the Eastern Mediterranean Basin. Shaded vertical bar corresponds to the ~56–44 ka wetter and warmer climate period. Abbreviations: BA = Bolling-Allerød; HE5 = Heinrich Event 5; LGM = Last Glacial Maximum; MIS = Marine Isotope Stage; S1=Sapropel 1; S3 = Sapropel 3; YD = Younger Dryas. Note the different percentage/values of vertical scales (after Langgut et al., 2018).

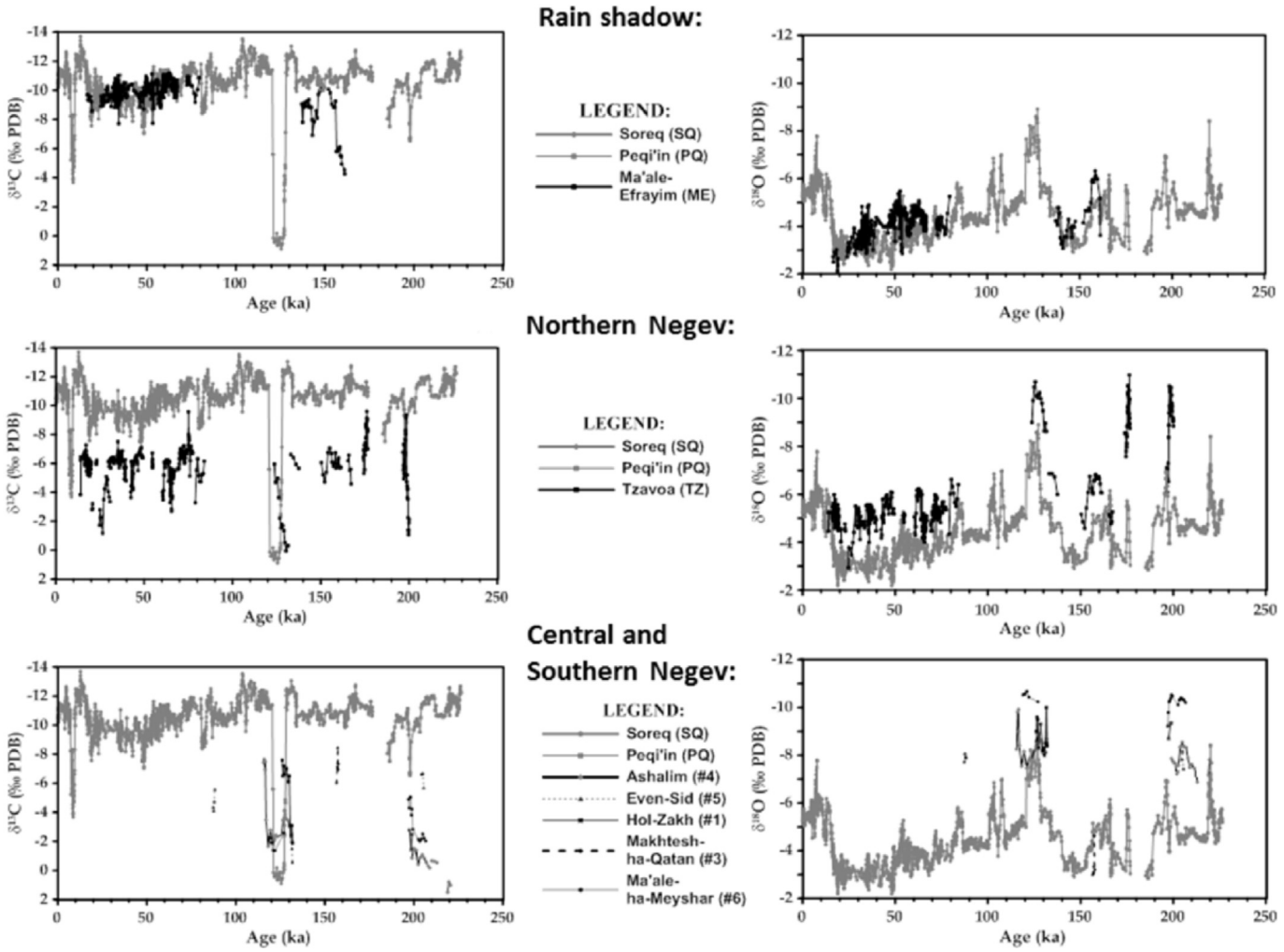

Fig. 6. The $\delta^{18}O$ and $\delta^{13}C$ records of speleothems from central segment of the DSB (ME Cave), Northern Negev (Tzavoa TZ cave – Vaks et al., 2006) and central and southern Negev caves (Vaks et al., 2010) superimposed on the $\delta^{18}O$ and $\delta^{13}C$ records of the Soreq and Peqi'in caves speleothems (Bar-Matthews et al., 2017).

indicated a major change from strong seasonality at ~125 ka BP (Torfstein and Enzel, 2017) with strong Mediterranean storm tracks, to weaker seasonality at 115 ka BP (Kutzbach et al., 2014). The enhanced winter contribution of rainfall was suggested to track from tropical Africa via tropical plumes as far north as the southern watershed of the DSB (Ziv et al., 2006; Kutzbach et al., 2014).

The speleothems $\delta^{13}C$ values show complicated features. During most of the interglacials, $\delta^{13}C$ values range between ~ -13.0‰ and ~-10.0‰, which is typical of dominant C3 type vegetation, but between 128 and 120 ka BP during MIS 5e, values rise to ~0‰. The minimum $\delta^{18}O$ values between 128.5-122 ka BP together with maximum $\delta^{13}C$ values were interpreted by Bar-Matthews et al. (2000, 2003) to reflect deluge events in which the dominant carbon source was weathering of the dolomitic host rock. This model is supported by the highest paleo pool levels in the cave (Bar-Matthews et al., 2003) and by the petrography and Sr isotopic composition of the speleothems, which point to increased host rock weathering (Ayalon et al., 1998). It is estimated that rainfall amount during this period could have been 20–70% higher compared to present-day (Bar-Matthews, 2014). High annual rainfall over the entire Mediterranean Basin is also interpreted from the speleothem record in the northern Levant, based on speleothems from Lebanon (Nehme et al., 2015; Verheyden et al., 2017), and also in distal regions, such as speleothems record from central Italy, Corchia and Renella caves (Zanchetta et al., 2007; Zhornyak et al., 2011), and the northern rim of the Alps (Spötl et al., 2010).

Frumkin et al. (2000) suggest that the high $\delta^{13}C$ between 128 and 120 ka BP could reflect unstable irregular high water flushing events with dry and warm conditions, loss of vegetation, and erosion of the soil cover. The flushing-floods must have been frequent enough to keep the pools full, and long enough for calcite deposition. Thus, we suggest that the deluge period was also characterized by increased frequency of rain events.

Less extreme conditions developed during the time between 109–100 ka BP and between 86-83ka BP, coinciding with the formation of sapropels S4 and S3. In between these sub-stages there is increase aridity in the region (e.g., Almogi-Labin et al., 2004) and $\delta^{18}O$ of speleothems are higher by 1–2‰ (Fig. 3), favoring increased aridity. Increased aridity is also indicated by the fact that speleothems from the northern Negev Desert ceased to grow (Figs. 2 and 6).

The Yammoûneh record indicates that forested landscapes developed in the Northern Levant with intense groundwater circulation. Here the wettest phases coincide with peak interglacial MIS 5e at 130–120 ka BP, MIS 5 b between 100 and 95 ka BP, and during MIS 5a between 85 and 73 ka BP (Develle et al., 2010, 2011).

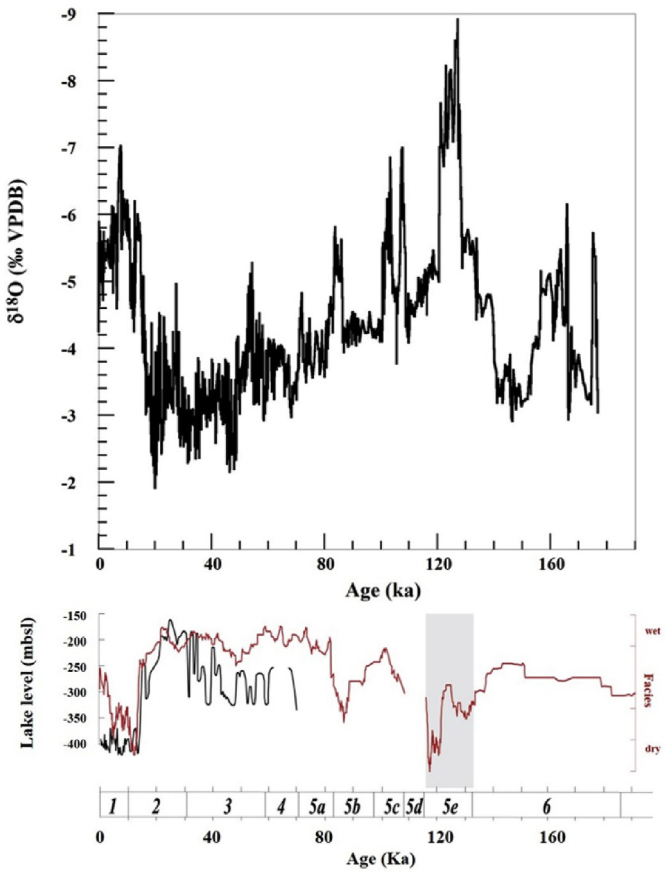

Fig. 7. Comparison between speleothems $\delta^{18}O$ record of Soreq Cave during the last 175 ka (Bar-Matthews et al., 2017) (top figure) and the Holocene Dead Sea and glacial Lake Lisan (Black line). The age normalized facies curve (marked in red) bottom figure (Torfstein et al., 2015).

2.2.3. Glacial conditions in the Northern Levant

Speleothem deposition in Jeita and Kannan caves did not occur during last glacial (Fig. 2) and even during deglaciation from 20 ka BP to 15 ka BP deposition was slow (Cheng et al., 2015; Nehme et al., 2015; Verheyden et al., 2017). On Mt Hermon (Mizpe Shelagim (MS) Cave, 2224 masl) at the southern end of the EM Alpine karst range, speleothem deposition was episodic (Figs. 2 and 5). Thus, the lack and/or episodic glacial speleothem deposition in the Northern Levant, suggests that the soil was frozen for most of the time, preventing water from infiltrating through the unsaturated zone. The short intervals of speleothems growth at the Mizpe Shelagim site occurred when average annual temperatures increased to >3 °C (Ayalon et al., 2013). These short intervals coincide with some of the Dansgaard-Oeschger events (Ayalon et al., 2013), with warming in the north eastern basin of the EMS (Almogi-Labin et al., 2009) and central and northern Israel, and with relatively humid glacial phases recorded in the Yammoûneh karstic Basin, northern Lebanon (Develle et al., 2010, 2011; Gasse et al., 2011).

2.2.4. Glacial conditions in the northern Negev Desert

In the northern Negev Desert, with present-day average annual rainfall amounts of ~200–300 mm, and no present-day deposition, speleothems were mainly deposited during glacial intervals, with deposition during peak interglacials (Figs. 2 and 6). Deposition during glacial periods suggests that the water balance in the northern Negev Desert was more positive compared to part of the interglacials and present-day. This observation is taken to indicate that the desert border migrated ~30 km southward from its present-day position (Fig. 8 in Vaks et al., 2006; Bar-Matthews et al., 2017). Comparison between the $\delta^{18}O$ and $\delta^{13}C$ values of the northern Negev Desert speleothems with central Israel speleothems show similar trend, but the absolute $\delta^{18}O$ values of the former are significantly lower and $\delta^{13}C$ values are higher (Fig. 6). The lower $\delta^{18}O$ values of the northern Negev speleothems most probably reflect Rayleigh distillation processes resulting from longer southward travel distance of rainfall (Vaks et al., 2006; Bar-Matthews et al., 2017). The higher $\delta^{13}C$ values in the northern Negev indicate that even during periods of increased northern Negev rainfall, the amounts were not enough to allow expansion of C3 type vegetation (Bar-Matthews et al., 2017). Thus, although speleothems were deposited during last glacial, the average amount of rainfall was lower compared to central and northern Israel.

2.2.5. Glacial conditions in the central and southern Negev Desert

A different picture emerges from central and southern Negev Desert speleothems, compared to the northern Negev Desert. In this part of the Negev Desert, which is the north-eastern extension of the large Saharo-Arabian Desert, no speleothems deposition occurred during last glacial, and only minor deposition occurred during MIS 6 (Figs. 2 and 6). Thus, while rainfall penetrated the northern Negev during glacial periods, the central and southern Negev remained dry.

2.2.6. Glacial conditions in the Dead Sea Basin

Before exploring the information derived from speleothems in this region, it is important to note that the very detailed study of Lake Lisan, the precursor of the Dead Sea, show that its highest stand occurred during the last glacial. It is argued that the existence of the larger Lake Lisan during glacial period compared with the Holocene Dead Sea requires significantly more rainfall (e.g., Zak, 1967; Begin et al., 1974; Bartov et al., 2003; Kolodny et al., 2005; Enzel et al., 2008). Begin et al. (2004) suggested that an additional southern rainfall source was more active during the last glacial, although this model has been not supported by additional evidence. The lake reached its highest stand and areal extent between ~27 ka BP and 23ka BP (Bartov et al., 2002, 2003; 2006, 2007; Haase-Schramm et al., 2004). However, this time interval is one for which a sediment core from the south-western shore of the Sea of Galilee shows that the predominant vegetation in northern Israel was steppe vegetation with grasses together and other herbs and dwarf shrubs, suggesting semi-arid conditions (Miebach et al., 2017). Thus, there is an apparent conflict between the pollen data, which call for relatively dry conditions during last glacial on one hand, and the high lake levels on the other hand, apparently pointing to much wetter conditions.

This raises the question of how the speleothems record from this relatively arid region responds to this duality.

Growth and non-growth patterns of speleothems present a picture of differences between the northern, central and southern segments of the DSB. In the northern section of the DSB, speleothems continuously deposited during glacial and interglacials, as evident from newly discovered Zalmon Cave speleothems (Fig. 1), where present-day annual rainfall is ~500 mm (Keinan et al., 2019, and Fig. 2). Their $\delta^{13}C$ values range for most of the time interval between −9 and −12‰, suggesting C3 type vegetation, similar to speleothems from central and northern Israel. However, their $\delta^{18}O$ values during the last glacial are lower by ~1–2‰ compared to central Israel caves (Keinan et al., 2019).

The offset to lower $\delta^{18}O$ values during glacials is interpreted to reflect two factors: Warmer temperatures coupled with increased rainfall amounts in the northern DSB relative to Soreq Cave area.

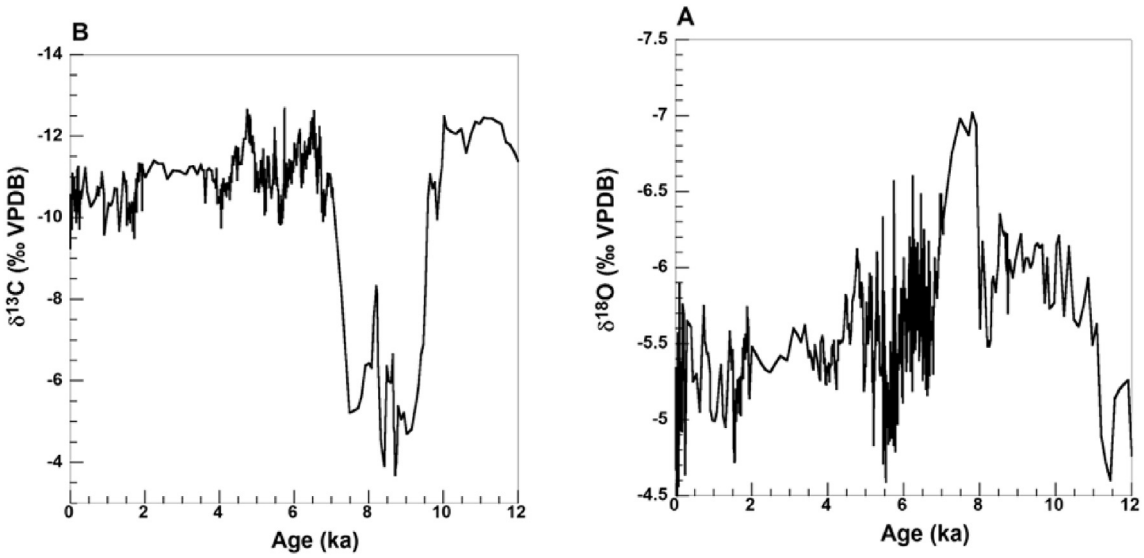

Fig. 8. $\delta^{18}O$ (A) and $\delta^{13}C$ (B) records of speleothems from Soreq Cave during the last 12 ka (Bar-Matthews et al., 2003, 2011; Grant et al., 2012).

The latter could be the result of the funneling of storm tracks from the Mediterranean Sea directly eastward across the Levant toward the northern DSB area (Keinan et al., 2019).

Farther south along the DSB where annual average amount of rainfall is below 250 mm, in ME Cave (Fig. 1), where no present-day speleothems deposition occurs, speleothems were mainly deposited during glacial periods, with only minor deposition during interglacial (Fig. 2). As with the northern Negev Desert, speleothems deposition during the last glacial suggests higher water availability in the central segment of the DSB relative to interglacials. However, unlike the northern Negev Desert speleothems, there is strong match between the $\delta^{18}O$ and $\delta^{13}C$ values of ME and Soreq Cave speleothems (Fig. 6), despite their being located 60 km apart, on the different sides of the CMR, and under very different present-day climates. This similarity indicates that during last glacial, the climate and vegetation were similar on both sides of the CMR, and rainfall that originated from the EMS source reached further east across the CMR (Vaks et al., 2003; Bar-Matthews et al., 2017). The similarity in climate and vegetation during glacials implies that the rainfall belt migrated at least 60 km farther east during last glacial and the amount of rainfall in both sides of the CMR was similar (Goldsmith et al., 2017), and with probably similar temperatures (McGarry et al., 2004).

Farther south, along the southern segment of the DSB, where annual rainfall is ~150-50 mm, speleothems deposition was very limited during last glacial with only very thin laminae, but their presence in this arid region during last glacial, indicates that more water was available relative to present (Lisker et al., 2010) (Fig. 2).

We therefore suggest that the high Lake Lisan stand during last glacial, mainly between 27 and 23 ka BP is not necessarily a good indicator for rainfall as the water balance. During last glacial climate conditions were much colder with average annual temperatures dropping to ~10 °C. The colder conditions, different relative humidity (Gat, 1996), and lower evaporation/precipitation ratio (Lisker et al., 2010; Vaks et al., 2003) in combination with short warm events that induced significant snow melting in the northern Levant during last glacial, would have drained large amounts of water into the DSB and recharged the ground water (Ayalon et al., 2013). All these most probably resulted in higher lake stand. Thus, the 'apparent' contradiction between 'wet' Dead Sea region, evident from the high Lake Lisan Stand (e.g. Torfstein et al., 2015 and Fig. 7), during most of last glacial on one hand, and a 'drier Mediterranean' based on the isotopic composition of the speleothems (Fig. 3), the EMS marine records (Fig. 3), and the pollen records (Fig. 5 and Langgut et al., 2011, 2018., Miebach et al., 2017; Chen and Litt, 2018) on the other hand, does not necessarily require greatly increased rainfall. It can be viewed as a different response of the lake system (Leng and Marshall, 2004; Roberts et al., 2008) to the combined effects of lower temperature, higher precipitation/evaporation ratio and additional water supply from the rainfall penetration farther east, additional rainfall to the northern DSB, and from snow melting from the northern Levant and possibly the high mountain area east of the DSB watershed (Bar-Matthews, 2014).

2.2.7. *Interglacial conditions in the central and southern Negev and the sources of rainfall to the southern and eastern Levant*

Evidence for wet peak interglacials, mainly MIS 5e in the Negev Desert, come from the timing of depositional periods of speleothems (Figs. 2 and 4) and from fossil corals in the elevated reef terraces along the Gulf of Aqaba which were extensively altered to calcite (Lazar and Stein, 2011; Yehudai et al., 2017). There is also evidence for wet conditions from freshwater deposits in the Arava Valley, Israel (Livnat and Kronfeld, 1985), and further south in Egypt from fossil groundwater carbonate spring deposits in oases in the Western Desert (Sultan et al., 1997), and secondary uranium in ores and carbonates, which indicate extreme ground water movement during Egyptian Sahara pluvial periods (Osmond and Dabous, 2004).

The view that emerges from central and southern Negev Desert speleothems (Vaks et al., 2010) is that this part of the Negev, which is the north-eastern extension of the large Saharo-Arabian Desert that became arid to hyperarid at ~1.0 Ma (Vaks et al., 2010; Amit et al., 2006; Enzel et al., 2008), experienced short pluvial periods during interglacials. The main evidence for this is the episodic deposition of speleothems with very thin laminae in dispersed sites (Figs. 2 and 4). The ages of their outermost layers show that deposition occurred mostly during interglacials.

The periods of speleothems deposition in the Negev Desert have been referred to as Negev Humid Periods (NHP) and must reflect intervals when rainfall amount was high enough to allow water to infiltrate the cave (Vaks et al., 2010; Bar-Matthews, 2014). High $\delta^{13}C$

values (Fig. 6) of these speleothems indicate that vegetation cover was not well established during these NHPs (Vaks et al., 2010; Bar-Matthews et al., 2017). Thus, it was proposed that these NHP's were clusters of short wet events during otherwise long droughts, sufficient to deposit a thin layer of carbonate in caves. This proposal is supported by the lack of calcic soil horizons in the southern Negev, which imply that these episodic wet events were neither intense nor prolonged (Amit et al., 2006).

Are the origin, amounts, and high frequency of rainfall during peak MIS 5e in the Negev Desert and in the Dead Sea Basin associated with increase intensity of EM cyclones and/or potentially associated with summer monsoonal rainfall, or both? Whereas Waldmann et al. (2009) and Torfstein et al. (2015) argue for enhanced rainfall associated with the African monsoon with mid subtropical latitude climate systems, Vaks et al. (2010) argue for increase intensity of EM cyclones that resulted in penetration of rainfall farther south. The latter argument was based on the reduced frequency of depositional episodes and thickness of individual speleothems laminae southwards, implying a decrease in rainfall from north to south, similar to the present-day precipitation gradient (Vaks et al., 2010). As in the Negev Desert, the most intensive speleothems deposition in Southern Arabia (Fig. 1) occurs during peak interglacials (Fig. 2). Fleitmann et al. (2011) argue that MIS 5e was the wettest interval with the main rain events being the African-Indian monsoon system.

Pluvial intervals recorded along the north-south transects from the Levant to southern Arabia (Fig. 1) may shed light on the origin of moisture. Rosenberg et al. (2013) show pluvial periods in the Nafud Desert Northern Arabia to be in phase with southern Negev speleothems (Vaks et al., 2010) and southern Arabia speleothems (Fleitmann et al., 2011). This temporal connection indicates intensive hydrological cycles over the entire Arabian Peninsula, but how far north the monsoonal storm track could reach is not clear. Whereas in southern Arabia the strengthening of the Indian monsoon was attributed to its intensification, the northern limit of the monsoonal migration is unknown, since currently, there is no current evidence for speleothems deposition in central Arabia (Fleitmann et al., 2003; Rosenberg et al., 2013).

The ability of monsoon-related southern-derived rains to directly impact the Negev Desert and the Dead Sea watershed is not trivial, considering the relatively high latitude of the DSB and southern and central Negev Desert caves and the distance from tropical Africa (Fig. 1). However, recent general circulation models (e.g., Herold and Lohmann, 2009) show significant northern excursions of summer monsoon rainfall, suggesting that the influence of the African monsoon could have reached as far north as the northern Arabian Peninsula**.** Other model results indicate that the enhanced winter contribution from tropical Africa via tropical plumes could have also affected the southern watershed of the Dead Sea (Kutzbach et al., 2014). However, enhanced precipitation from southern sources to the Levant during MIS 5e is still not well understood.

2.2.8. The Holocene (MIS 1)

The transition from the LGM, ~19 ka BP to MIS 1 is gradual and characterized by $\delta^{18}O$ decrease from ~-2.0‰ to −6.0‰ and $\delta^{13}C$ decrease from ~-7.00‰ to ~-13.0‰ (Fig. 3), with several short peaks coinciding with the Heinrich 1, Bolling-Allerod and the Younger Dryas events. The Early Holocene, between 9.4 and 7.0 ka BP, is characterized by low speleothem $\delta^{18}O$ values coupled with the very high $\delta^{13}C$ values (Fig. 8) that coincide with the deposition of sapropel S1 (e.g., Bar-Matthews et al., 2000), and points to a very wet early Holocene. There is no speleothems deposition in the "rain shadow" desert or in the entire Negev Desert, Israel (Fig. 2), suggesting that rainfall did not penetrate during the very wet early Holocene to these desert areas, and the overall present-day climate zones of the EM - Levant region were already established during early Holocene. The Dead Sea level dropped to −400 mbsl (Fig. 7).

Early Holocene wet conditions also characterize the northern Red Sea and it was suggested by Arz et al. (2003) that Mediterranean moisture source reached this far south. Penetration of Mediterranean moisture source is not evident from the Negev Desert, since there is no speleothems deposition. However, the combined records of speleothems from Oman and Yemen show continuous growth during the Holocene (Fleitmann et al., 2007 and Fig. 2) suggesting that the contribution of moisture source to the northern Red Sea may derive from southern source. The $\delta^{18}O$ record of Arabia and Yemen speleothems show northward displacement of the ITCZ during early Holocene, and during middle-late Holocene, the summer ITCZ gradually migrated southward and monsoon precipitation decreased (Fleitmann et al., 2007).

Whereas the early Holocene is considered to be very wet, the mid-late Holocene period is characterized by the present-day climatic seasonality pattern of wet winters and dry summers (Orland1 et al., 2009; 2012), and also by significant rapid climate changes (Mayewski et al., 2004) that are mainly associated with changes in rainfall amount between average annual precipitation of ~800 mm and ~300 mm (Bar-Matthews and Ayalon, 2011). Several short-lived decadal-to centennial-scale climatic events were identified during the mid-Holocene. Dry events occurred at 6.65–6.60 ka BP, 6.25–6.18 ka BP, 5.70–5.6 ka BP, 5.25–5.17 ka BP and 4.2–4.05 ka BP. The last two events coincided with the cultural collapse of the Uruk society in Mesopotamia and the Akkadian Empire. Short climatic wet events occurred at 6.70–6.68 ka BP, 6.17–6.10 ka BP, 5.76–5.74 ka BP, and 5.50–5.45 ka BP (Bar-Matthews and Ayalon, 2011).

3. Conclusions

The climate system of the mid-latitude EM - Levant region is linked to the North-Atlantic climate system on one hand and the African subtropical monsoon system on the other hand. This results in a unique climate response to regional and global climate changes. The speleothems research made on numerous caves in the region show that most of last glacial was relatively cold and dry, but that the rainfall system from the EMS penetrated further east by about 60 km, and about 30 km further south.

During peak interglacials, mainly MIS 5e, central and northern Israel experienced deluge rainfall conditions. High frequency rainfall events also associated with the westerlies penetrated farther south to the northern Negev Desert during peak interglacials. The central and southern Negev Desert, and to some extent the Dead Sea Basin experienced clusters of short wet events during otherwise long drought periods. A still remaining important issue that is not clearly resolved is the importance of Monsoon-derived rainfall in the Levant. Speleothem records tell us that the main rainfall source in the EMS - Levant region was moisture derived from the EMS surface. This conclusion appears to hold in the southern parts of the Negev Desert, where thinning and increased scarcity of speleothem favors a northward rainfall source. In this case, the monsoon only contributes indirectly to EMS - Levant rainfall $\delta^{18}O$ source through the input of monsoonal generated freshwater from River Nile. Studies of the DSBDDP core have, however, suggested that the Monsoon rainfall may move north into the Dead Sea Basin. Thus, the relative importance of these two rainfall sources still needs to be resolved through further studies. The overall present-day climate zones of the EM - Levant region were established during mid-late Holocene.

Acknowledgments

The cave research was supported by Israel Science Foundation (grants 20/01–13.0 and 910/05) and by the United States-Israel Binational Science Foundation (2008158 and 2010316). We thank the Geological Survey of Israel for the support given to the work, and the Israeli Nature and Parks Authority for their cooperation. We would like to thank Tami Zilberman and Alan Matthews for their fruitful discussions. We thank the two anonymous reviewers and the editor Neil Roberts for their constructive comments that highly improved the manuscript.

References

Affek, H.P., Bar-Matthews, M., Ayalon, A., Matthews, A., Eiler, J.M., 2008. Glacial/interglacial temperature variations in Soreq cave speleothems as recorded by 'clumped isotope' thermometry. Geochem. Cosmochim. Acta 72, 5351–5360. https://doi.org/10.1016/j.gca.2008.06.031.

Almogi-Labin, A., Bar-Matthews, M., Ayalon, A., 2004. Climate variability in the Levant and northeast Africa during the Late Quaternary based on marine and land records. In: Goren-Inbar, Naama, Speth, John D. (Eds.), Human Paleoecology in the Levantine Corridor. Oxbow Press, Oxford, pp. 117–134.

Almogi-Labin, A., Bar-Matthews, M., Shriki, D., Kolosovsky, E., Paterne, M., Schilman, B., Ayalon, A., Aizenshtat, Z., Matthews, A., 2009. Climatic variability during the last ~90ka of the southern and northern Levantine Basin as evident from marine records and speleothems. Quat. Sci. Rev. 28, 2882–2896. https://doi.org/10.1016/j.quascirev.2009.07.017.

Amit, R., Enzel, Y., Sharon, D., 2006. Permanent Quaternary hyperaridity in the Negev, Israel, resulting from regional tectonics blocking Mediterranean frontal systems. Geology 34, 509–512.

Arz, H.W., Lamy, F., Pä tzold, J., Muller, P.J., Prins, M., 2003. Mediterranean moisture source for an early-Holocene humid period in the northern Red Sea. Science 300, 118–121.

Ayalon, A., Bar-Matthews, M., Sass, E., 1998. Rainfall-recharge relationships within a karstic terrain in the Eastern Mediterranean semi-arid region, Israel: δ 18O and δD characteristics. J. Hydrol. 207, 18–31. https://doi.org/10.1016/S0022-1694(98)00119-X.

Ayalon, A., Bar-Matthews, M., Kaufman, A., 1999. Petrography, strontium, barium and uranium concentrations, and strontium and uranium isotope ratios in speleothems as palaeoclimatic proxies: Soreq Cave, Israel. Holocene 9, 715–722. https://doi.org/10.1191/095968399673664163.

Ayalon, A., Bar-Matthews, M., Kaufman, A., 2002. Climatic conditions during marine oxygen isotope stage 6 in the eastern Mediterranean region from the isotopic composition of speleothems of Soreq Cave. Israel: Geology 30, 303–306. https://doi.org/10.1130/0091-7613(2002)030<0303:CCDMOI>2.0.CO.

Ayalon, A., Bar-Matthews, M., Schilman, B., 2004. Rainfall Isotopic Characteristics in Various Vites in Israel and the Relationships with the Unsaturated Zone Water.

Ayalon, A., Bar-Matthews, M., Frumkin, A., Matthews, A., 2013. Last Glacial warm events on Mount Hermon: the southern extension of the Alpine karst range of the east Mediterranean. Quat. Sci. Rev. 59, 43–56. https://doi.org/10.1016/j.quascirev.2012.10.047.

Bar-Matthews, M., 2014. History of water in the Middle East and north Africa. In: Treatise on Geochemistry. Elsevier, pp. 109–128. https://doi.org/10.1016/B978-0-08-095975-7.01210-9.

Bar-Matthews, M., Ayalon, A., 2011. Mid-Holocene climate variations revealed by high resolution speleothem records from Soreq Cave, Israel and their correlation with cultural changes. Holocene 21, 163–171.

Bar-Matthews, M., Ayalon, A., Kaufman, A., 1997. Late quaternary paleoclimate in the eastern mediterranean region from stable isotope analysis of speleothems at Soreq cave, Israel. Quat. Res. 47, 155–168. https://doi.org/10.1006/qres.1997.1883.

Bar-Matthews, M., Ayalon, A., Kaufman, A., 1998. Palaeoclimate evolution in the eastern Mediterranean region during the last 58,000 years as derived from stable isotopes of speleothems (Soreq Cave, Israel): Isotope Techniques in the Study of the Environmental Change, pp. 673–682.

Bar-Matthews, M., Ayalon, A., Kaufman, A., 2000. Timing and hydrological conditions of Sapropel events in the Eastern Mediterranean, as evident from speleothems, Soreq cave, Israel. Chem. Geol. 169, 145–156. https://doi.org/10.1016/S0009-2541(99)00232-6.

Bar-Matthews, M., Ayalon, A., Gilmour, M., Matthews, A., Hawkesworth, C.J., 2003. Sea–land oxygen isotopic relationships from planktonic foraminifera and speleothems in the Eastern Mediterranean region and their implication for paleorainfall during interglacial intervals. Geochem. Cosmochim. Acta 67, 3181–3199. https://doi.org/10.1016/S0016-7037(02)01031-1.

Bar-Matthews, M., Ayalon, A., Vaks, A., Frumkin, A., 2017. Climate and environment reconstructions based on speleothems from the levant. In: Enzel, Y., Bar-Yosef, O. (Eds.), Quaternary of the Levant. Cambridge University Press, Cambridge, pp. 151–164. https://doi.org/10.1017/9781316106754.017.

Bartov, Y., Stein, M., Enzel, Y., Agnon, A., Reches, Z., 2002. lake levels and sequence stratigraphy of Lake lisan, the late pleistocene precursor of the Dead Sea. Quat. Res. 57, 9–21. https://doi.org/10.1006/qres.2001.2284.

Bartov, Y., Goldstein, S.L., Stein, M., Enzel, Y., 2003. Catastrophic arid episodes in the eastern mediterranean linked with the north atlantic Heinrich events. Geology 31, 439–442.

Bartov, Y., Bookman, R., Enzel, Y., 2006. Current Depositional Environments at the Dead Sea Margins as Indicators of Past Lake Levels, vol. 2401. Geological Society of America, pp. 127–140. https://doi.org/10.1130/2006.2401(08.

Bartov, Y., Enzel, Y., Porat, N., Stein, M., 2007. Evolution of the late pleistocene Holocene Dead Sea basin from sequence stratigraphy of fan deltas and lake-level reconstruction. J. Sediment. Res. 77, 680–692.

Begin, Z.B., Ehrlich, A., Nathan, Y., 1974. Lake Lisan, the pleistocene precursor of the Dead Sea. Geol. Surv. Isr. Bull. 63, 30.

Begin, Z.B., Stein, M., Katz, A., Machlus, M., Rosenfeld, A., Buchbinder, B., Bartov, Y., 2004. Southward migration of rain tracks during the last glacial, revealed by salinity gradient in Lake Lisan (Dead Sea rift). Quat. Sci. Rev. 23, 1627–1636.

Burns, S.J., Matter, A., Frank, N., Mangini, A., 1998. Speleothem-based paleoclimate record from northern Oman. Geology 26, 499–502.

Burns, S.J., Fleitmann, D., Matter, A., Neff, U., Mangini, A., 2001. Speleothem evidence from Oman for continental pluvial events during interglacial periods. Geology 29, 623–626.

Cheddadi, R., Rossignol-Strick, M., 1995a. Eastern Mediterranean Quaternary paleoclimates from pollen and isotope records of marine cores in the Nile cone area. Paleoceanograp. Paleoclimatol. 10, 291–300.

Cheddadi, R., Rossignol-Strick, M., 1995b. Improved preservation of organic matter and pollen in eastern Mediterranean sapropels. Paleoceanography 10, 301–309.

Chen, C., Litt, T., 2018. Dead Sea pollen provides new insights into the paleoenvironment of the southern Levant during MIS 6–5. Quat. Sci. Rev. 188, 15–27.

Cheng, H., Sinha, A., Verheyden, S., Nader, F.H., Li, X.L., Zhang, P.Z., Yin, J.J., Yi, L., Peng, Y.B., Rao, Z.G., Ning, Y.F., Edwards, R.L., 2015. The climate variability in northern Levant over the past 20,000 years. Geophys. Res. Lett. https://doi.org/10.1002/2015GL065397.

Cita, M.B., Vergnaud-Grazzini, C., Robert, C., Chamley, H., Ciaranfi, N., d'Onofrio, S., 1977. Paleoclimatic record of a long deep sea core from the eastern Mediterranean. Quat. Res. 8, 205–235.

Develle, A.-L., Herreros, J., Vidal, L., Sursock, A., Gasse, F., 2010. Controlling factors on a paleo-lake oxygen isotope record (Yammoûneh, Lebanon) since the Last Glacial Maximum. Quat. Sci. Rev. 29, 865–886. https://doi.org/10.1016/j.quascirev.2009.12.005.

Develle, A.-L., Gasse, F., Vidal, L., Williamson, D., Demory, F., Van Campo, E., Ghaleb, B., Thouveny, N., 2011. A 250ka sedimentary record from a small karstic lake in the Northern Levant (Yammoûneh, Lebanon). Palaeogeogr. Palaeoclimatol. Palaeoecol. 305, 10–27. https://doi.org/10.1016/j.palaeo.2011.02.008.

Emeis, K.-C., Schulz, H.-M., Struck, U., Sakamoto, T., Doose, H., Erlenkeuser, H., Howell, M., Kroon, D., Paterne, M., 1998. Stable isotope and alkenone temperature records of sapropels from Sites 964 and 967: constraining the physical environment of sapropel formation in the Eastern Mediterranean Sea. In: Proceedings of the Ocean Drilling Program, 160 Scientific Results, Ocean Drilling Program. https://doi.org/10.2973/odp.proc.sr.160.011.1998.

Emeis, K.-C., Sakamoto, T., Wehausen, R., Brumsack, H.-J., 2000a. The sapropel record of the eastern Mediterranean Sea—results of ocean drilling program leg 160. Palaeogeogr. Palaeoclimatol. Palaeoecol. 158, 371–395.

Emeis, K.-C., Struck, U., Schulz, H.-M., Rosenberg, R., Bernasconi, S., Erlenkeuser, H., Sakamoto, T., Martinez-Ruiz, F., 2000b. Temperature and salinity variations of Mediterranean Sea surface waters over the last 16,000 years from records of planktonic stable oxygen isotopes and alkenone unsaturation ratios. Palaeogeogr. Palaeoclimatol. Palaeoecol. 158, 259–280.

Emeis, K., Schulz, H., Struck, U., Rossignol-Strick, M., Erlenkeuser, H., Howell, M.W., Kroon, D., Mackensen, A., Ishizuka, S., Oba, T., 2003. Eastern Mediterranean surface water temperatures and δ18O composition during deposition of sapropels in the late Quaternary. Paleoceanograp. Paleoclimatol. 18.

Enzel, Y., Amit, R., Dayan, U., Crouvi, O., Kahana, R., Ziv, B., Sharon, D., 2008. The climatic and physiographic controls of the eastern Mediterranean over the late Pleistocene climates in the southern Levant and its neighboring deserts. Glob. Planet. Chang. 60, 165–192. https://doi.org/10.1016/j.gloplacha.2007.02.003.

Essallami, L., Sicre, M.A., Kallel, N., Labeyrie, L., Siani, G., 2007. Hydrological changes in the Mediterranean Sea over the last 30,000 years. Geochem. Geophys. Geosyst. 8.

Fleitmann, D., Burns, S.J., Neff, U., Mangini, A., Matter, A., 2003. Changing moisture sources over the last 330,000 years in Northern Oman from fluid-inclusion evidence in speleothems. Quat. Res. 60, 223–232. https://doi.org/10.1016/S0033-5894(03)00086-3.

Fleitmann, D., Burns, S.J., Mangini, A., Mudelsee, M., Kramers, J., Villa, I., Neff, U., Al-Subbary, A.A., Buettner, A., Hippler, D., Matter, A., 2007. Holocene ITCZ and Indian monsoon dynamics recorded in stalagmites from Oman and Yemen (Socotra). Quat. Sci. Rev. 26, 170–188.

Fleitmann, D., Burns, S.J., Pekala, M., Mangini, A., Al-Subbary, A., Al-Aowah, M., Kramers, J., Matter, A., 2011. Holocene and Pleistocene pluvial periods in Yemen, southern Arabia. Quat. Sci. Rev. 30, 783–787. https://doi.org/10.1016/j.quascirev.2011.01.004.

Fontugne, M.R., Calvert, S.E., 1992. Late pleistocene variability of the carbon isotopic composition of organic matter in the eastern mediterranean: monitor of changes in carbon sources and atmospheric CO 2 concentrations. Paleoceanography 7, 1–20. https://doi.org/10.1029/91PA02674.

Frumkin, A., Ford, D.C., Schwarcz, H.P., 1999. Continental oxygen isotopic record of the last 170,000 Years in Jerusalem. Quat. Res. 51, 317–327. https://doi.org/

10.1006/qres.1998.2031.
Frumkin, A., Ford, D.C., Schwarcz, H.P., 2000. Paleoclimate and vegetation of the last glacial cycles in Jerusalem from a speleothem record. Glob. Biogeochem. Cycles 14, 863–870. https://doi.org/10.1029/1999GB001245.
Frumkin, A., Bar-Yosef, O., Schwarcz, H.P., 2011. Possible paleohydrologic and paleoclimatic effects on hominin migration and occupation of the Levantine Middle Paleolithic. J. Hum. Evol. 60, 437–451. https://doi.org/10.1016/j.jhevol.2010.03.010.
Gasse, F., Vidal, L., Develle, A.-L., Campo, E. Van, 2011. Hydrological variability in the Northern Levant: a 250 ka multiproxy record from the Yammôuneh (Lebanon) sedimentary sequence. Clim. Past 7.
Gat, J.R., 1996. Oxygen and hydrogen isotopes in the hydrologic cycle. Annu. Rev. Earth Planet Sci. 24, 225–262. https://doi.org/10.1007/s00170-012-4640-z.
Gat, J.R., Carmi, I., 1987. Effect of Climate Changes on the Precipitation Patterns and Isotopic Composition of Water in a Climate Transition Zone : Case of the Eastern Mediterranean Sea Area: the Influence of Climate Change and Climatic Variability on the Hydrologic Regime and Water Resources. In: (Proceedings of the Vancouver Symposium, August 1987). IAHS Publ., pp. 513–524. https://doi.org/10.1016/j.foodchem.2014.06.060
Goldsmith, Y., Polissar, P.J., Ayalon, A., Bar-Matthews, M., Broecker, W.S., 2017. The modern and Last Glacial Maximum hydrological cycles of the Eastern Mediterranean and the Levant from a water isotope perspective. Earth Planet. Sci. Lett. 457, 302–312.
Grant, K.M., Rohling, E.J., Bar-Matthews, M., Ayalon, A., Medina-Elizalde, M., Ramsey, C.B., Satow, C., Roberts, A.P., 2012. Rapid coupling between ice volume and polar temperature over the past 150,000 years. Nature 491, 744–747. https://doi.org/10.1038/nature11593.
Grant, K.M., Grimm, R., Mikolajewicz, U., Marino, G., Ziegler, M., Rohling, E.J., 2016. The timing of Mediterranean sapropel deposition relative to insolation, sea-level and African monsoon changes. Quat. Sci. Rev. 140, 125–141. https://doi.org/10.1016/j.quascirev.2016.03.026.
Gvirtzman, H., 2002. Israel Water Resources. Yad Ben-Zvi Press, Jerusalem, p. 287.
Haase-Schramm, A., Goldstein, S.L., Stein, M., 2004. U-Th dating of Lake Lisan (late Pleistocene Dead Sea) aragonite and implications for glacial East Mediterranean climate change. Geochem. Cosmochim. Acta 68, 985–1005.
Herold, M., Lohmann, G., 2009. Eemian tropical and subtropical African moisture transport: an isotope modelling study. Clim. Dyn. 33, 1075–1088.
Hershkovitz, I., Marder, O., Ayalon, A., Bar-Matthews, M., Yasur, G., Boaretto, E., Caracuta, V., Alex, B., Frumkin, A., Goder-Goldberger, M., Gunz, P., Holloway, R.L., Latimer, B., Lavi, R., et al., 2015. Levantine cranium from Manot Cave (Israel) foreshadows the first European modern humans. Nature 520, 216–219. https://doi.org/10.1038/nature14134.
Hilgen, F.J., 1991. Astronomical calibration of Gauss to Matuyama sapropels in the Mediterranean and implication for the geomagnetic polarity time scale. Earth Planet. Sci. Lett. 104, 226–244.
Kahana, R., Ziv, B., Enzel, Y., Dayan, U., 2002. Synoptic climatology of major floods in the Negev Desert, Israel. Int. J. Climatol. 22, 867–882. https://doi.org/10.1002/joc.766.
Kallel, N., Paterne, M., Duplessy, J.C., Vergnaudgrazzini, C., Pujol, C., Labeyrie, L., Arnold, M., Fontugne, M., Pierre, C., 1997a. Enhanced rainfall in the Mediterranean region during the last sapropel event. Oceanol. Acta 20, 697–712.
Kallel, N., Paterne, M., Labeyrie, L., Duplessy, J.-C., Arnold, M., 1997b. Temperature and salinity records of the Tyrrhenian Sea during the last 18,000 years. Palaeogeogr. Palaeoclimatol. Palaeoecol. 135, 97–108.
Keinan, J., Bar-Matthews, M., Ayalon, A., Zilberman, T., Agnon, A., Frumkin, A., 2019. Paleoclimatology of the levant from Zalmon cave speleothems, the northern Jordan valley, Israel. Quat. Sci. Rev. (in press).
Kolodny, Y., Stein, M., Machlus, M., 2005. Sea-rain-lake relation in the last glacial east mediterranean revealed by δ18O-δ13C in Lake Lisan aragonites. Geochem. Cosmochim. Acta 69, 4045–4060. https://doi.org/10.1016/j.gca.2004.11.022.
Kotthoff, U., Pross, J., Müller, U.C., Peyron, O., Schmiedl, G., Schulz, H., Bordon, A., 2008. Climate dynamics in the borderlands of the Aegean Sea during formation of sapropel S1 deduced from a marine pollen record. Quat. Sci. Rev. 27, 832–845.
Kushnir, Y., Cassou, C., St George, S., 2017. Editorial: decadal climate variability. Past Global Chang. Magaz. 25 https://doi.org/10.22498/pages.25.1.1, 1–1.
Kutzbach, J.E., Chen, G., Cheng, H., Edwards, R.L., Liu, Z., 2014. Potential role of winter rainfall in explaining increase moisture in the Mediterranean and Middle East during periods of maximum orbitally-forced insolation seasonality. Clim. Dyn. 42, 1079–1095.
Langgut, D., 2008. Late Quaternary Palynological Sequences from the Eastern Mediterranean Sea: Jerusalem Report. Geological Survey of Israel.
Langgut, D., Almogi-Labin, A., Bar-Matthews, M., Weinstein-Evron, M., 2011. Vegetation and climate changes in the South Eastern Mediterranean during the last glacial cycle (86 ka): a new marine pollen record. Quat. Sci. Rev. 30, 3960–3972.
Langgut, D., Almogi-Labin, A., Bar-Matthews, M., Pickarski, N., Weinstein-Evron, M., 2018. Evidence for a humid interval at~ 56–44 ka in the Levant and its potential link to modern humans dispersal out of Africa. J. Hum. Evol. 124, 75–90.
Lazar, B., Stein, M., 2011. Freshwater on the route of hominids out of Africa revealed by U-Th in Red Sea corals. Geology 39, 1067–1070.
Leng, M.J., Marshall, J.D., 2004. Palaeoclimate interpretation of stable isotope data from lake sediment archives. Quat. Sci. Rev. 23, 811–831.
Lionello, P., Malanotte-izzoli, P., Boscolo, R., Alpert, P., Artale, V., Li, L., Luterbacher, J., May, W., Trigo, R., Tsimplis, M., Ulbrich, U., Xoplaki, E., 2006. The Mediterranean climate: an overview of the main characteristics and issues. Develop. Earth Environ. Sci. 4, 1–26.
Lisiecki, L.E., Raymo, M.E., 2005. A Pliocene-Pleistocene stack of 57 globally distributed benthic δ18O records. Paleoceanography 20, 1.
Lisker, S., Vaks, A., Bar-Matthews, M., Porat, R., Frumkin, A., 2009. Stromatolites in caves of the Dead Sea Fault Escarpment: implications to latest Pleistocene lake levels and tectonic subsidence. Quat. Sci. Rev. 28, 80–92. https://doi.org/10.1016/j.quascirev.2008.10.015.
Lisker, S., Vaks, A., Bar-Matthews, M., Porat, R., Frumkin, A., 2010. Late Pleistocene palaeoclimatic and palaeoenvironmental reconstruction of the Dead Sea area (Israel), based on speleothems and cave stromatolites. Quat. Sci. Rev. 29 (9–10), 1201–1211.
Livnat, A., Kronfeld, J., 1985. Paleoclimatic implications of U-series dates for lake sediments and travertines in the Arava Rift Valley, Israel. Quat. Res. 24, 164–172.
Lourens, L.J., Antonarakou, A., Hilgren, F.J., van Hoof, A.A.M., Vergnaud-Grazzini, C., Zachariasse, W.J., 1996. Evaluation of the Plio-Pleistocene astronomical timescale. Paleoceanography 11, 391–413, 11, 391–413.
Marino, G., Rohling, E.J., Sangiorgi, F., Hayes, A., Casford, J.L., Lotter, A.F., Kucera, M., Brinkhuis, H., 2009. Early and middle Holocene in the Aegean Sea: interplay between high and low latitude climate variability. Quat. Sci. Rev. 28, 3246–3262.
Matthews, A., Ayalon, A., Bar-Matthews, M., 2000. D/H ratios of fluid inclusions of Soreq Cave (Israel) speleothems as a guide to the Eastern Mediterranean Meteoric Line relationships in the last 120 ky. Chem. Geol. 166, 183–191.
Mayewski, P.A., Rohling, E.E., Stager, J.C., Karlen, W., Maascha, K.A., Meekler, L.D., et al., 2004. Holocene climate variability. Quat. Res. 62, 243–255.
McGarry, S., Bar-Matthews, M., Matthews, A., Vaks, A., Schilman, B., Ayalon, A., 2004. Constraints on hydrological and paleotemperature variations in the Eastern Mediterranean region in the last 140ka given by the δD values of speleothem fluid inclusions. Quat. Sci. Rev. 23, 919–934. https://doi.org/10.1016/j.quascirev.2003.06.020.
Miebach, A., Chen, C., Schwab, M.J., Stein, M., Litt, T., 2017. Vegetation and climate during the Last Glacial high stand (ca. 28–22 ka BP) of the Sea of Galilee, northern Israel. Quat. Sci. Rev. 156, 47–56. https://doi.org/10.1016/j.quascirev.2016.11.013.
Nehme, C., Verheyden, S., Noble, S.R., Farrant, A.R., Sahy, D., Hellstrom, J., Delannoy, J.J., Claeys, P., 2015. Reconstruction of MIS 5 climate in the central Levant using a stalagmite from Kanaan Cave, Lebanon. Clim. Past 11, 1785–1799. https://doi.org/10.5194/cp-11-1785-2015.
Orland, I.J., Bar-Matthews, M., Ayalon, A., Matthews, A., Kozdon, R., Ushikubo1, T., Valley, J.W., 2012. Seasonal resolution of Eastern Mediterranean climate change since 34 ka from a Soreq Cave speleothem. Geochem. Cosmochim. Acta 89, 240–255.
Orland, I.J., Bar-Matthews, M., Kita, N.T., Ayalon, A., Matthews, A., Valley, J.W., 2009. Climate deterioration in the eastern Mediterranean as revealed by ion microprobe analysis of a speleothem that grew from 2.2 to 0.9 ka in Soreq Cave, Israel. Quat. Res. 71, 27–35.
Osborne, A.H., Vance, D., Rohling, E.J., Barton, N., Rogerson, M., Fello, N., 2008. A humid corridor across the Sahara for the migration of early modern humans out of Africa 120,000 years ago. Proc. Natl. Acad. Sci. 105, 16444–16447.
Osborne, A.H., Marino, G., Vance, D., Rohling, E.J., 2010. Eastern Mediterranean surface water Nd during Eemian sapropel S5: monitoring northerly (mid-latitude) versus southerly (sub-tropical) freshwater contributions. Quat. Sci. Rev. 29, 2473–2483.
Osmond, J.K., Dabous, A.A., 2004. Timing and intensity of groundwater movement during Egyptian Sahara pluvial periods by U-series analysis of secondary U in ores and carbonates. Quat. Res. 61, 85–94.
Rindsberger, M., Magaritz, M., Carmi, I., Gilad, D., 1983. The relation between air mass trajectories and the water isotope composition of rain in the Mediterranean Sea area. Geophys. Res. Lett. 10, 43–46. https://doi.org/10.1029/GL010i001p00043.
Roberts, N., Jones, M.D., Benkaddour, A., Eastwood, W.J., Filippi, M.L., Frogley, M.R., Lamb, H.F., Leng, M.J., Reed, J.M., Stein, M., 2008. Stable isotope records of Late Quaternary climate and hydrology from Mediterranean lakes: the ISOMED synthesis. Quat. Sci. Rev. 27, 2426–2441.
Rodríguez-Sanz, L., Bernasconi, S.M., Marino, G., Heslop, D., Mueller, I.A., Fernandez, A., Grant, K.M., Rohling, E.J., 2017. Penultimate deglacial warming across the Mediterranean Sea revealed by clumped isotopes in foraminifera. Sci. Rep. 7, 16572.
Rohling, E.J., Cane, T.R., Cooke, S., Sprovieri, M., Bouloubassi, I., Emeis, K.C., Schiebel, R., Kroon, D., Jorissen, F.J., Lorre, A., 2002. African monsoon variability during the previous interglacial maximum. Earth Planet. Sci. Lett. 202, 61–75.
Rohling, E.J., Marino, G., Grant, K.M., 2015. Mediterranean climate and oceanography, and the periodic development of anoxic events (sapropels). Earth Sci. Rev. 143, 62–97.
Rosenberg, T.M., Preusser, P., Risberg, J., Plikk, A., Kadi, K.A., Matter, A., Fleitmann, D., 2013. Middle and Late Pleistocene humid periods recorded in palaeolake deposits of the Nafud desert, Saudi Arabia. Quat. Sci. Rev. 70, 109–123.
Rossignol-Strick, M., 1983. African monsoons, an immediate climate response to orbital insolation. Nature 304, 46.
Rossignol-Strick, M., 1985. Mediterranean Quaternary sapropels, an immediate response of the African monsoon to variation of insolation. Palaeogeogr. Palaeoclimatol. Palaeoecol. 49, 237–263.
Rossignol-Strick, M., Nesteroff, W., Olive, P., Vergnaud-Grazzini, C., 1982. After the deluge: Mediterranean stagnation and sapropel formation. Nature 295, 105.
Rozanski, K., Araguás-Araguás, L., Gonfiantini, R., 1993. Isotopic Patterns in Modern

Global Precipitation: Climate Change in Continental Isotopic Records, vol. 78, pp. 1–36.
Rubin, S., Ziv, B., Paldor, N., 2007. Tropical plumes over eastern North Africa as a source of rain in the Middle East. Mon. Weather Rev. 135, 4135–4148. https://doi.org/10.1175/2007MWR1919.1.
Scrivner, A.E., Vance, D., Rohling, E.J., 2004. New neodymium isotope data quantify Nile involvement in Mediterranean anoxic episodes. Geology 32, 565–568.
Sharon, D., Kutiel, H., 1986. The distribution of rainfall intensity in Israel, its regional and seasonal variations and its climatological evaluation. J. Climatol. 6, 277–291. https://doi.org/10.1002/joc.3370060304.
Spötl, C., Nicolussi, K., Patzelt, G., Boch, R., 2010. Humid climate during deposition of sapropel 1 in the Mediterranean Sea: assessing the influence on the Alps. Glob. Planet. Chang. 71, 242–248.
Sultan, M., Sturchio, N., Hassan, F.A., Hamdan, M.A.R., Mahmood, A.M., El Alfy, Z., Stein, T., 1997. Precipitation source inferred from stable isotopic composition of Pleistocene groundwater and carbonate deposits in the Western desert of Egypt. Quat. Res. 48, 29–37.
Terink, W., Immerzeel, W., Droogers, P., 2013. Climate change projections of precipitation and reference evapotranspiration for the Middle East and Northern Africa until 2050. Int. J. Climatol. https://doi.org/10.1002/joc.3650.
Torfstein, A., Enzel, Y., 2017. Dead Sea lake level changes and levant paleoclimate. In: Enzel, Y., Bar-Yosef, O. (Eds.), Quaternary of the Levant: Environments, Climate Change, and Humans. Cambridge University Press, Cambridge, pp. 115–125.
Torfstein, A., Goldstein, S., Kagan, E.J., Stein, M., 2013. Integrated multi-site U–Th chronology of the last glacial Lake Lisan. Geochem. Cosmochim. Acta 210–231.
Torfstein, A., Goldstein, S.L., Kushnir, Y., Enzel, Y., Haug, G., Stein, M., 2015. Dead Sea drawdown and monsoonal impacts in the Levant during the last interglacial. Earth Planet. Sci. Lett. 412, 235–244. https://doi.org/10.1016/j.epsl.2014.12.013.
Tsvieli, Y., Zangvil, A., 2007. Synoptic climatological analysis of Red Sea trough and non-Red Sea trough rain situations over Israel. Adv. Geosci. 12, 137–143. https://doi.org/10.5194/adgeo-12-137-2007.
Vaks, A., Bar-Matthews, M., Ayalon, A., Schilman, B., Gilmour, M., Hawkesworth, C.J., Frumkin, A., Kaufman, A., Matthews, A., 2003. Paleoclimate reconstruction based on the timing of speleothem growth and oxygen and carbon isotope composition in a cave located in the rain shadow in Israel. Quat. Res. 59, 182–193. https://doi.org/10.1016/S0033-5894(03)00013-9.
Vaks, A., Bar-Matthews, M., Ayalon, A., Matthews, A., Frumkin, A., Dayan, U., Halicz, L., Almogi-Labin, A., Schilman, B., 2006. Paleoclimate and location of the border between Mediterranean climate region and the Saharo–Arabian Desert as revealed by speleothems from the northern Negev Desert, Israel. Earth Planet. Sci. Lett. 249 (3–4), 384–399.
Vaks, A., Bar-Matthews, M., Ayalon, A., Matthews, A., Halicz, L., Frumkin, A., 2007. Desert speleothems reveal climatic window for African exodus of early modern humans. Geology 35, 831–834. https://doi.org/10.1130/G23794A.1.
Vaks, A., Bar-Matthews, M., Matthews, A., Ayalon, A., Frumkin, A., 2010. Middle-late quaternary paleoclimate of northern margins of the saharan-Arabian desert: reconstruction from speleothems of Negev desert, Israel. Quat. Sci. Rev. 29, 2647–2662. https://doi.org/10.1016/j.quascirev.2010.06.014.
Vaks, A., Mason, A.J., Breitenbach, S.F.M., Kononov, A.M., Osintcev, A.V., Henderson, G.M., 2014. 1,100,000 year history of Siberian permafrost based on U-Pb chronology of speleothems. In: EGU General Assembly Conference Abstracts, vol. 16.
Verheyden, S., Nehme, C., Nader, F.H., Farrant, A.R., Cheng, H., Noble, S.R., Sahy, D., Edwards, R.L., Swennen, R., Claeys, P., Delannoy, J.J., 2017. Speleothems from Lebanon. In: Bar-Yosef, O., Enzel, Y. (Eds.), Quaternary of the Levant. Cambridge University Press, Cambridge, pp. 165–172. https://doi.org/10.1017/9781316106754.018.
Waldmann, N., Stein, M., Ariztegui, D., Starinsky, A., 2009. Stratigraphy, depositional environments and level reconstruction of the last interglacial Lake Samra in the Dead Sea basin. Quat. Res. 72, 1–15. https://doi.org/10.1016/j.yqres.2009.03.005.
Yehudai, M., Lazar, B., Bar, N., Kiro, Y., Agnon, A., Shaked, Y., Stein, M., 2017. U–Th dating of calcite corals from the Gulf of Aqaba. Geochem. Cosmochim. Acta 198, 285–298.
Zak, I., 1967. The Geology of Mount Sedom. The Hebrew University of Jerusalem. PhD theisi.
Zanchetta, G., Drysdale, R.N., Hellstrom, J.C., Fallick, A.E., Isola, I., Gagan, M.K., Pareschi, M.T., 2007. Enhanced rainfall in the Western Mediterranean during deposition of sapropel S1: stalagmite evidence from Corchia cave (Central Italy). Quat. Sci. Rev. 26, 279–286.
Zhornyak, L.V., Zanchetta, G., Drysdale, R.N., Hellstrom, J.C., Isola, I., Regattieri, E., Piccini, L., Baneschi, I., Couchoud, I., 2011. Stratigraphic evidence for a "pluvial phase" between ca 8200–7100 ka from Renella cave (Central Italy). Quat. Sci. Rev. 30, 409–417.
Ziv, B., 2001. A subtropical rainstorm associated with a tropical plume overAfrica and the Middle-East. Theor. Appl. Climatol. 69, 91–102. https://doi.org/10.1007/s007040170037.
Ziv, B., Dayan, U., Kushnir, Y., Roth, C., Enzel, Y., 2006. Regional and global atmospheric patterns governing rainfall in the southern Levant. Int. J. Climatol. 26, 55–73.